

THE NATURE OF LINERS^a

^aOBSERVATIONS REPORTED IN THIS PAPER WERE OBTAINED WITH THE MULTIPLE MIRROR TELESCOPE, WHICH IS OPERATED JOINTLY BY THE SMITHSONIAN ASTROPHYSICAL OBSERVATORY AND THE UNIVERSITY OF ARIZONA.

ALMUDENA ALONSO-HERRERO, MARCIA J. RIEKE, GEORGE H. RIEKE
Steward Observatory, The University of Arizona, Tucson, AZ 85721

AND

JOSEPH C. SHIELDS
Department of Physics and Astronomy, Ohio University, Athens, OH 45701-2979
Draft version August 13, 2018

ABSTRACT

We present J -band ($1.15 - 1.35 \mu\text{m}$) spectroscopy of a sample of nine galaxies showing some degree of LINER activity (classical LINERs, weak-[O I] LINERs and transition objects), together with H -band spectroscopy for some of them. A careful subtraction of the stellar continuum allows us to obtain reliable [Fe II]1.2567 μm /Pa β line ratios. We conclude that different types of LINERs (i.e., photoionized by a stellar continuum or by an AGN) cannot be easily distinguished based solely on the [Fe II]1.2567 μm /Pa β line ratio.

The emission line properties of many LINERs can be explained in terms of an aging starburst. The optical line ratios of these LINERs are reproduced by a model with a metal-rich H II region component photoionized with a single stellar temperature $T_* = 38,000$ K, plus a supernova remnant (SNR) component. The [Fe II] line is predominantly excited by shocks produced by SNRs in starbursts and starburst-dominated LINERs, while Pa β tracks H II regions ionized by massive young stars. The contribution from SNRs to the overall emission line spectrum is constrained by the [Fe II]1.2567 μm /Pa β line ratio. Although our models for aging starbursts are constrained only by these infrared lines, they consistently explain the optical spectra of the galaxies also.

The LINER-starburst connection is tested by predicting the time dependence of the ratio of the ionizing luminosity (L_{ion}) to the supernova rate (SNr), $L_{\text{ion}}/(\text{SNr})$. We predict the relative number of starbursts to starburst-dominated LINERs (aging starbursts) and show that it is in approximate agreement with survey findings for nearby galaxies.

Subject headings: Galaxies: active – galaxies: nuclei – galaxies: stellar content – infrared: galaxies

1. INTRODUCTION

Low ionization nuclear emission line regions (LINERs, Heckman 1980) are probably the most common type of galaxy nuclear activity; 1/3 of all spiral galaxies with $B < 12.5$ show LINER spectra (Ho, Filippenko, & Sargent 1993, 1997b). LINERs, however, appear to be a heterogeneous class of objects (Heckman 1986). The detection of a broad H α component in some ($\sim 24\%$) LINERs (Ho et al. 1993, 1997b), the presence of unresolved UV sources in a few objects (Maoz et al. 1995) and the continuity of X-ray properties from the luminous active Seyferts to low-luminosity active galaxies (Koratkar et al. 1995) suggest that in some LINERs photoionization by a non-stellar continuum (AGN) source is the dominant excitation process. However LINER spectra can also be modeled by photoionization by hot stars in a dense medium (Shields 1992; Filippenko & Terlevich 1992). The similarity of some LINER spectra to those of supernova remnants initially suggested that the optical lines of LINERs could be excited by shock heated gas (Heckman 1980) caused by supernovae or from AGN-associated processes.

Engelbracht et al. (1998) show in detail how the LINER characteristics of the weak-[O I] LINER/H II galaxy NGC 253 arise unavoidably from an old nuclear

starburst, as its hot stars fade and a high supernova rate persists. Other authors have proposed less specific connections between LINER emission-line characteristics and late phase starbursts. For example, Larkin et al. (1998) suggest that a number of classical LINERs have Pa β absorption stronger than would be expected for a pure old stellar population, indicating the presence of a significant number of hotter stars. Maoz et al. (1998) find that UV spectra of LINERs can show stellar absorption lines, suggesting that the emission of some LINERs with compact UV sources could be unrelated to the presence of a low luminosity AGN.

Infrared and extreme emission line galaxies appear to be undergoing starbursts with a duration of ~ 10 million years (Rieke et al. 1993; Genzel et al. 1995; Engelbracht et al. 1996, 1998; Böker, Förster-Schreiber, & Genzel 1997; Vanzi, Alonso-Herrero, & Rieke 1998). As starbursts age, they should fade to become Balmer absorption galaxies. However, the intermediate age starbursts ($\sim 20 - 40$ million years old) have not been found in significant numbers. The modeling by Engelbracht et al. (1998) suggests that many of these galaxies have been masquerading as LINERs. The goal of this study is to test this connection by making use of near-IR spectroscopy and additional model-

TABLE 1
THE SAMPLE OF LINERs.

Galaxy (1)	v_{hel} (km s^{-1}) (2)	Run (3)	t_{exp} (s) (4)	Nuclear Type (5)	Reference optical (6)	Reference infrared (7)
NGC 2639	3336	Dec 1996	2880	LINER	1,2,7	a
NGC 3031 (M81)	-34	Dec 1996	1440	LINER	1,2	b
NGC 3367	3037	Dec 1996	1920	weak-LINER	1,3	a
NGC 3504	1539	Dec 1996	1440	weak-LINER	1,2	a
NGC 3998	1040	Dec 1996	2160	LINER	1,2,7	a
NGC 4569 (M90)	-235	Dec 1996	2880	weak-LINER	1,4,7	c
NGC 4579 (M58)	1519	Apr 1997	2160	LINER	1,5,7	a
NGC 5953	1965	Apr 1997	2160	LINER/Sy2/SB	6	a
NGC 7743	1710	Dec 1996	1920	LINER/Sy2	1,2	a
NGC 3379	920	Mar 1997	2160	E (template)

NOTE.—Col. (1) Galaxy. Col. (2) Heliocentric velocity from NED. Col. (3) Observing run for the near-IR spectroscopy. Col. (4) Integration time for the J -band spectroscopy. Integration times for H -band spectra: NGC 3367 5760 s and 4320 s, NGC 3504 4320 s (intermediate resolution) and 1680 s (high resolution), NGC 4569 1440 s and NGC 7743 1920 s. Col. (5) Nuclear type, see Appendix for more details on the classification. Cols.(6) References for the optical line ratios: 1. Ho et al. (1997a) 2. Ho et al. (1993) 3. Véron-Cetty & Véron (1986) and Véron et al. (1997) 4. Stauffer (1982) 5. González-Delgado & Pérez (1996b) 6. Veilleux et al. (1995). 7. Keel (1983). Col. (7) References for the infrared aperture photometry: a. This work b. Forbes et al. (1992) c. Devereux et al. (1987)

ing of a sample of nearby LINERs. In Section 2 we describe the sample and the observations. In Section 3, we derive near-infrared and optical line ratios and show that in many cases they agree with expectations for aging starbursts. In Section 4 we show that the LINER-starburst connection predicts a plausible number of LINERs to agree with observation. Our conclusions are presented in Section 5.

2. OBSERVATIONS

2.1. The sample

We present in this study near-infrared spectroscopy of a sample of galaxies showing some degree of LINER activity. Due to the heterogeneous nature of the LINER class we have adopted the following initial criteria for the classification. We selected candidates from Ho et al. (1993) and Ho et al. (1995); for the latter reference, the LINER classification was confirmed with optical line ratios found elsewhere in the literature (references given in Table 1). We classified a galaxy as a *pure* (or classical) LINER only if it fully satisfies Heckman’s (1980) definition ($[\text{O II}]\lambda 3727 > [\text{O III}]\lambda 5007$ and $[\text{O I}]\lambda 6300 > 0.3[\text{O III}]\lambda 5007$). Weak- $[\text{O I}]\lambda 6300$ LINERs were taken to have the line ratio $[\text{O I}]\lambda 6300/\text{H}\alpha < 1/6$ (Filippenko & Terlevich 1992). Other galaxies can be classified as transition objects because they show a composite H II/LINER spectra. In addition, the activity classification seems to be aperture dependent for some objects in our sample. In the Appendix we give more details on the classification of each galaxy, since in some cases the determination of the LINER class is not straightforward.

For the initial sample we used the $\text{H}\alpha$ fluxes from the literature to determine what galaxies might have a detectable level of $\text{Pa}\beta$ emission at our resolution. Our sample is therefore biased toward relatively bright emission line galaxies. Such a bias is inevitable for an infrared spectroscopic sample, since the $\text{Pa}\beta$ line is intrinsically an order of magnitude weaker than $\text{H}\beta$ and a normal galaxy

continuum at constant spectral resolution is an order of magnitude brighter at $\text{Pa}\beta$ than at $\text{H}\beta$, so the emission line spectrum is detectable in the infrared only for strong-lined galaxies.

For the purposes of this study we will also include the near-infrared spectroscopic data of the LINER prototype NGC 1052 (Alonso-Herrero et al. 1997), the weak- $[\text{O I}]$ LINER NGC 253 (Engelbracht et al. 1998), the classical LINER/Wolf-Rayet galaxy NGC 6764 (Calzetti 1997), and the sample of LINERs presented in Larkin et al. (1998).

2.2. Near-Infrared Spectroscopy

We obtained near-infrared long-slit spectra in the J -band ($1.15 - 1.35 \mu\text{m}$) of nine LINERs at the Multiple Mirror Telescope (MMT) with the infrared spectrometer FSPEC (Williams et al. 1993) during two observing runs in 1996 December and 1997 April. For both observing runs we used a slit of $1''.2 \times 30''$ with pixel size $0''.4 \text{ pixel}^{-1}$ and a 300 groove mm^{-1} grating which provides a resolution of $\lambda/\Delta\lambda \simeq 460$ at $1.25 \mu\text{m}$. In addition to the spectra of the LINERs, a J -band spectrum of the elliptical galaxy NGC 3379, to be used as a template, was obtained at the Steward Observatory 61-Inch telescope on 1997 March 26, with pixel size $1''.8 \text{ pixel}^{-1}$ and a slit two pixels wide.

Observations were obtained for each galaxy at three or four positions along the slit, integrating for 2 or 4 minutes at each position. This pattern was repeated until the desired signal to noise was achieved (at least 40, if possible). Approximately solar-type stars were observed in a similar fashion, interspersed with the galaxy observations, and selected to be at similar air masses. The data reduction process involves dark current subtraction, flat-fielding and sky subtraction. The correction for atmospheric transmission is performed by dividing the galaxy spectrum by the adjacent spectrum of the standard star. The resulting spectrum is multiplied by a solar spectrum to correct

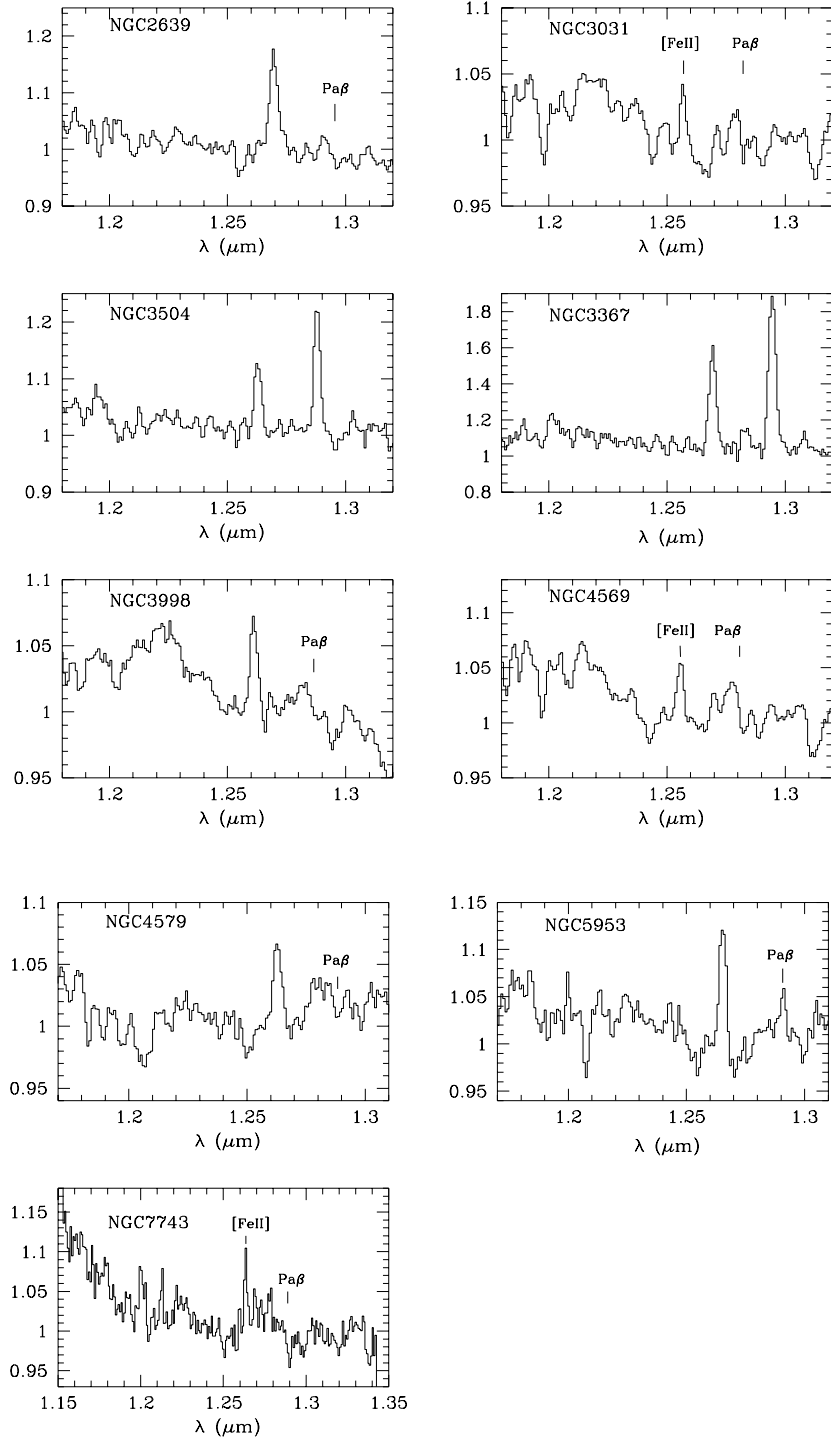


FIG. 1.— Observed J -band spectra of the LINERs normalized to unity. The extraction aperture is $1.2'' \times 2''$ in all cases. The $[\text{Fe II}]1.257 \mu\text{m}$ is clearly detected in all spectra.

for the standard star absorption features (as described by Maiolino, Rieke, & Rieke 1996). The wavelength calibration was performed by making use of OH sky lines from the list in Oliva & Origlia (1992).

Additional spectra at resolution $\lambda/\Delta\lambda \simeq 750$ in the H -band ($1.65 \mu\text{m}$) were obtained for NGC 3367, NGC 3504 and NGC 4569 on the 1996 Dec run. A high resolution ($\lambda/\Delta\lambda \simeq 1500$) spectrum in the H -band ($\lambda = 1.68 \mu\text{m}$) of NGC 3504 was also obtained on the night of 1996 June 1 which will be combined with the $\lambda = 1.63 \mu\text{m}$ spectra presented in Alonso-Herrero et al. (1997). Similar observational and reduction procedures were used throughout.

In Table 1 we present the sample of galaxies: column (3) gives the observing run for each galaxy, and column (4) the total integration time in seconds for the J -band spectra. The integration times for the H spectra are given in the notes.

2.3. Near-Infrared Imaging and Flux-Calibration of the IR Spectra

Because of the small projected width of the slit and the unknown slit losses, we flux calibrated the spectra with images. We obtained broad-band images through J , H and K s filters with a NICMOS3 array at the Steward Observatory 90" telescope on Kitt Peak for seven galaxies in our sample on the nights of 1997 January 15 (NGC 2639 and NGC 7743), 1997 May 24 (NGC 3367), 1998 January 14 (NGC 5953+NGC 5954 only in J and K and NGC 4957 only in J), 1998 April 14 (NGC 3504 only J band) and 1998 November 6 (NGC 3998 J and K). For all observing runs the pixel size was $0''.6 \text{ pixel}^{-1}$. The data were reduced following a standard procedure which basically involves dark subtraction, flat fielding, shifting of the galaxy images to a common position and median-combining to produce the final image. Standard stars from the list of Elias et al. (1982) were observed several times throughout the night to provide a photometric calibration for the 1997 January and 1998 November data. We used the standard extinction coefficients for the site; errors from the photometric calibration are $\pm 0.06, 0.07$ and 0.06 mag at J , H and K respectively. Conditions were non-photometric in the 1997 May, 1998 January and 1998 April runs, so the images had to be calibrated with published fluxes. For NGC 3367 we used the $15''$ -diameter photometry given in Spinoglio et al. (1995), for the interacting pair NGC 5953+NGC 5954 we used the $5.5''$ -diameter photometry from Bushouse & Stanford (1992), for NGC 4579 the $5.5''$ -diameter photometry of Devereux, Becklin & Scoville (1987), and finally for NGC 3504 the $10''$ -diameter photometry from Balzano & Weedman (1981). The integration times for each filter along with the aperture photometry for these galaxies are presented in Table 2.

The flux-calibration of the near-IR spectra was performed using the $3''$ -diameter photometry from the images (Table 2), which approximately corresponds to the region covered by the large extraction aperture ($1.2'' \times 6''$), except NGC 3504 for which we used a $1.2'' \times 8.5''$ aperture to match that of our data in Alonso-Herrero et al. (1997), and NGC 3998 for which a $1.2'' \times 4''$ approximately matches the aperture of Larkin et al. (1998). The small aperture spectra ($1.2'' \times 2''$) were flux-calibrated relative to the large

aperture spectra. The spectra of NGC 3031, NGC 3504 and NGC 4569 were calibrated with aperture photometry from the literature (see references in Table 1, column (7)).

3. ANALYSIS

In Figure 1 we present the fully reduced J -band spectra, normalized to unity (at $1.25 \mu\text{m}$). These spectra were extracted with an aperture of $1.2'' \times 2''$. The $[\text{Fe II}]1.2567 \mu\text{m}$ line is clearly detected in all cases, whereas the $\text{Pa}\beta$ line is not detected in NGC 3998, NGC 7743, and is probably seen in absorption in NGC 2639, NGC 3031, NGC 4569 and NGC 4579. For the galaxies in which $\text{Pa}\beta$ is not detected, its expected location is indicated, inferred from the observed wavelength of $[\text{Fe II}]1.2567 \mu\text{m}$. Table 3 lists for each galaxy the line measurements for the apertures used to flux calibrate the spectra (given in the second column) in the first row, whereas the second row gives the same quantities for a $1.2'' \times 2''$ aperture. When $\text{Pa}\beta$ was not observed in emission an upper limit is tabulated. The full widths at half maximum (FWHM) are corrected for the instrument resolution ($\text{FWHM}_{\text{inst}} \simeq 650 \text{ km s}^{-1}$ at $1.25 \mu\text{m}$, as derived from the sky line widths). The J -band emission lines of NGC 3031, NGC 3367, NGC 3504, NGC 4569 and NGC 7743 appear unresolved at our resolution, while the other galaxies have marginally resolved lines. Due to the uncertainties of the continuum placement, the line fluxes, particularly of $\text{Pa}\beta$, are uncertain. For the two galaxies in common with Larkin et al. (1998), we measure a $[\text{Fe II}]1.257 \mu\text{m}$ flux three times as large as they do for NGC 3998, whereas given the differing aperture sizes, the $[\text{Fe II}]1.257 \mu\text{m}$ fluxes for NGC 7743 are consistent.

3.1. Stellar continuum subtraction

The strong stellar continuum dominates the J -band spectra of all our LINERs but NGC 3367. To improve the estimates of line strengths, we have used a "template" spectrum to subtract this continuum. Our template is produced from a spectrum of the elliptical galaxy NGC 3379 combined with our off-nuclear spectrum of M81. The former galaxy is often used for similar purposes in the optical, and the latter spectrum samples the stellar population actually present close to a LINER nucleus. The spectra are shown at the bottom of Figure 2. These spectra have been normalized by fitting the slope of the continuum. Within the errors, there is no difference in the two template components. The $\text{Pa}\beta$ line is observed in absorption with equivalent width $\text{EW} = -1.6 \text{ \AA}$ together with a number of absorption features (see below). We also display the solar spectrum¹ between 1.15 and $1.35 \mu\text{m}$, rebinned to our spectral resolution (top spectrum in Figure 2). We give possible identifications from Livingston & Wallace (1991) and Striganov & Sventinskii (1968) for some of the absorptions, as indicated in Figure 2 and summarized in Table 4. The wavelengths quoted are the average of the measured wavelengths in all the spectra where the feature is observed (the galaxies in which a given feature is seen are listed in the last column).

We shifted the LINER spectra to the rest wavelength, normalized them to unity, and then subtracted the J -band template. The stellar continuum subtracted spectra of our LINERs are presented in Figure 3, correspond-

¹NSO/Kitt Peak FTS data used here were produced by NSF/NOAO

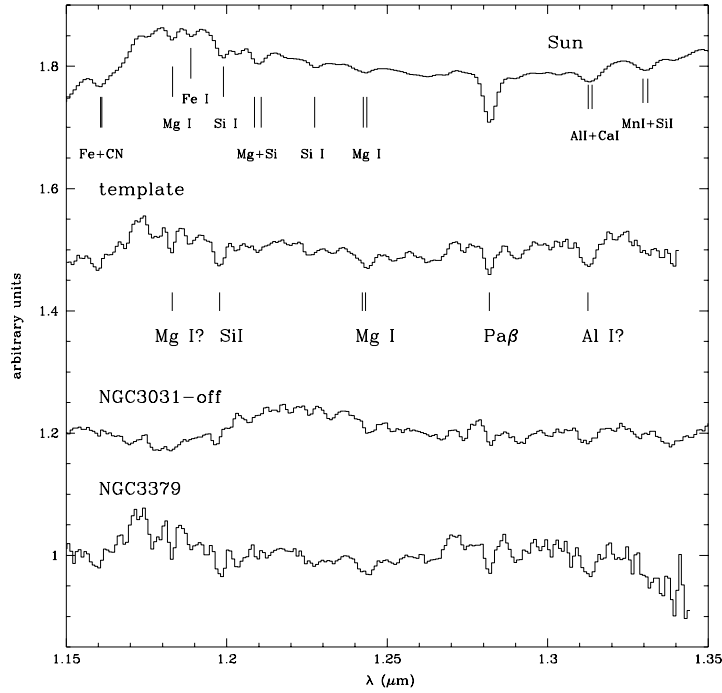


FIG. 2.— From bottom to top, J -band spectrum of the elliptical galaxy NGC 3379, off-nucleus of NGC 3031, the result of combining the previous galaxies (template spectrum), and the sun (rebinned to our spectral resolution). The spectra of NGC 3379, off-nucleus NGC 3031 and template have been shifted to the rest-frame wavelength. We mark the absorption features identified in the solar spectrum, and the tentative identifications in the template spectrum.

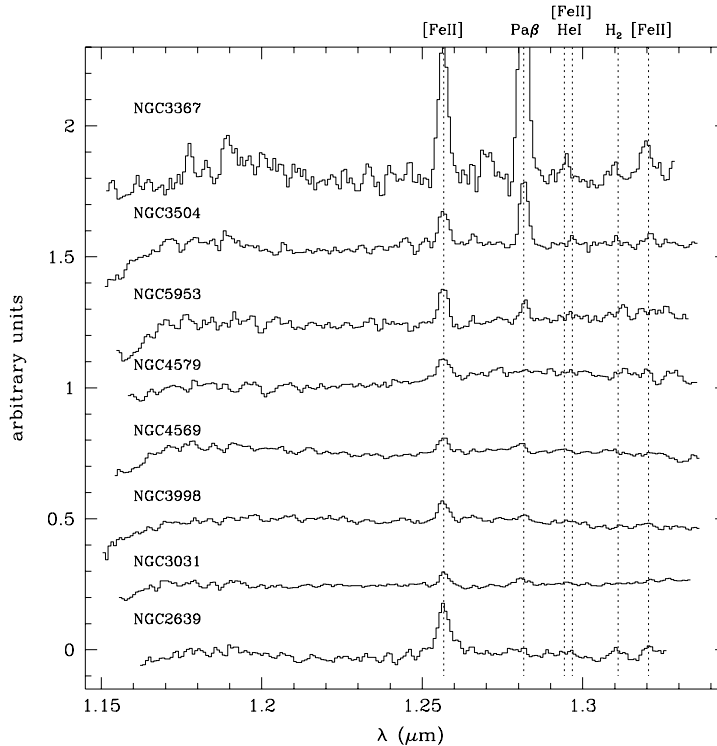


FIG. 3.— Stellar continuum subtracted spectra ($1.2'' \times 2''$ aperture) in the J -band shifted to the rest-frame wavelength. The spectra have been moved up by an arbitrary amount for displaying purposes. We indicate the position of $[\text{Fe II}]1.256 \mu\text{m}$ and $\text{Pa}\beta$. Also marked possible detections of the emission lines $[\text{Fe II}]1.2943 \mu\text{m}$ and $\text{He I}\lambda 1.2968 \mu\text{m}$, $\text{H}_2(4,2)\text{S}(1)\lambda 1.3112 \mu\text{m}$ and $[\text{Fe II}]1.3205 \mu\text{m}$.

TABLE 2
NEAR-INFRARED APERTURE PHOTOMETRY.

Galaxy	t_{int}	Diameter ($''$)	$J - H$	$J - K$	J
NGC 2639	J 540 s	3	0.96	1.23	12.85
	H 480 s	6	0.93	1.22	11.85
	K 600 s	9	0.92	1.18	11.34
		12	0.93	1.19	11.01
		15	0.93	1.19	10.77
NGC 3367		30	0.93	1.19	10.15
	J 480 s	3	0.80	1.22	14.02
	H 600 s	6	0.85	1.14	13.14
	K 600 s	9	0.84	1.10	12.66
		12	0.83	1.08	12.34
NGC 3504		15	0.83	1.06	12.12
		30	0.77	1.01	11.30
		45	0.74	1.00	10.79
	J 600 s	3	12.16
		6	11.17
NGC 3998		9	10.81
		12	10.61
		15	10.47
		30	10.05
	J 300 s	3	...	1.12	10.00
NGC 4579	K 300 s	6	...	1.06	9.11
		9	...	1.05	8.72
		12	...	1.04	8.48
		15	...	1.04	8.31
		30	...	1.02	7.93
NGC 5953	J 300 s	3	11.69
	K 300 s	6	10.76
		9	10.31
		12	10.01
		15	9.78
NGC 5954		30	9.12
	J 300 s	3	...	1.26	12.84
	K 300 s	6	...	1.13	11.89
		9	...	1.11	11.47
		12	...	1.09	11.21
NGC 5954		15	...	1.08	11.06
		30	...	1.05	10.73
	J 300 s	3	...	1.29	14.75
	K 300 s	6	...	1.14	13.70
		9	...	1.11	13.13
NGC 7743		12	...	1.08	12.74
		15	...	1.06	12.48
		30	...	1.01	11.74
	J 600 s	3	0.70	1.10	12.56
	H 600 s	6	0.70	1.05	11.81
NGC 7743	K 600 s	9	0.69	1.02	11.45
		12	0.69	1.00	11.21
		15	0.68	0.99	11.03
		30	0.65	0.94	10.49

TABLE 3
J-BAND SPECTRAL FEATURES.

Galaxy	Aperture	[Fe II] 1.257 μm	Pa β				
(1)	(2)	flux (3)	EW (4)	FWHM (5)	flux (6)	EW (7)	FWHM (8)
NGC 2639	1.2'' \times 6''	1.38×10^{-14}	6.1	675	$< 2 \times 10^{-15}$
	1.2'' \times 2''	1.14×10^{-14}	8.0	675	$< 1 \times 10^{-15}$
NGC 3031	1.2'' \times 6''	2.73×10^{-14}	1.1	< 650	$< 1 \times 10^{-14}$
	1.2'' \times 2''	1.80×10^{-14}	1.5	< 650	$< 6 \times 10^{-15}$
NGC 3367	1.2'' \times 6''	1.28×10^{-14}	16.0	< 650	2.11×10^{-14}	26.9	< 650
	1.2'' \times 2''	8.18×10^{-15}	21.6	< 650	1.34×10^{-14}	33.5	< 650
NGC 3504	1.2'' \times 8.5''	3.80×10^{-14}	5.3	< 650	8.03×10^{-14}	11.1	< 650
	1.2'' \times 2''	1.45×10^{-14}	4.3	< 650	2.42×10^{-14}	7.2	< 650
NGC 3998	1.2'' \times 4''	1.60×10^{-14}	2.5	< 650	$< 4 \times 10^{-15}$
	1.2'' \times 2''	1.10×10^{-14}	2.9	< 650	$< 4 \times 10^{-15}$
NGC 4569	1.2'' \times 8.5''	1.70×10^{-14}	1.4	< 650	$< 7 \times 10^{-15}$
	1.2'' \times 2''	1.42×10^{-14}	1.8	< 650	$< 3 \times 10^{-15}$
NGC 4579	1.2'' \times 6''	1.76×10^{-14}	2.6	875	$< 5 \times 10^{-15}$
	1.2'' \times 2''	1.20×10^{-14}	3.4	875	$< 3 \times 10^{-15}$
NGC 5953	1.2'' \times 6''	1.10×10^{-14}	4.8	< 650	7.97×10^{-15}	2.8	< 650
	1.2'' \times 2''	6.70×10^{-15}	4.7	< 650	3.05×10^{-15}	2.3	< 650
NGC 7743	1.2'' \times 6''	5.63×10^{-15}	3.2	< 650	$< 9 \times 10^{-16}$

NOTE.—Col. (1) Galaxy. Col. (2) Extraction aperture. Col. (3) and (6) Fluxes in $\text{erg cm}^{-2} \text{s}^{-1}$ measured from observed spectra (before stellar continuum subtraction). Col. (4) and (7) EW in \AA . Col. (5) and (8) FWHM in km s^{-1} (corrected for instrumental resolution).

TABLE 4
 ABSORPTION FEATURES OBSERVED IN THE *J*-BAND TEMPLATE SPECTRUM.

λ_{obs} (1)	Species (2)	λ_{vac} (3)	Galaxies (4)	Comment (5)
$1.1828 \pm 0.004 \mu\text{m}$	Mg I	$1.1828 \mu\text{m}$	NGC 2639, NGC 3031, NGC 3504 ? NGC 4569, NGC 5953	a
$1.1885 \pm 0.004 \mu\text{m}$	Fe I	$1.1886 \mu\text{m}$	NGC 2639 ?, NGC 3031, NGC 4569	a
$1.1978 \pm 0.004 \mu\text{m}$	Si I	1.1984, 1.1991 μm	NGC 2639, NGC 3031, NGC 3504? NGC 3998, NGC 4569, NGC 4579	a
$1.2433 \pm 0.004 \mu\text{m}$	Mg I	1.2424, 1.2433 μm	NGC 2639, NGC 3031, NGC 3998	b
	K I	$1.2432 \mu\text{m}$	NGC 4569, NGC 4579, NGC 5953	c, d
$1.3126 \pm 0.004 \mu\text{m}$	Al I	$1.3123 \mu\text{m}$	NGC 3031, NGC 3504?, NGC 3367 ?	
	Ca I	$1.3135 \mu\text{m}$	NGC 3998?, NGC 4569	d

NOTE.—Col. (1) Observed wavelength of the feature in the template spectrum. Col. (2) and (3) Tentative identification and vacuum wavelength. Col. (4) Galaxies in which the feature is tentatively detected. Col. (5) Comments.

a. The Mg I $\lambda 1.1828 \mu\text{m}$, and the Fe I lines have been identified in the spectra of cool low-mass stars (Jones et al. 1996).

b. The Mg I doublet is identified in LINERs (Larkin et al. 1998).

c. The K I line is present in M dwarf stars (Kirkpatrick et al. 1993).

d. The Ca I line is identified in M stars (Jones et al. 1994).

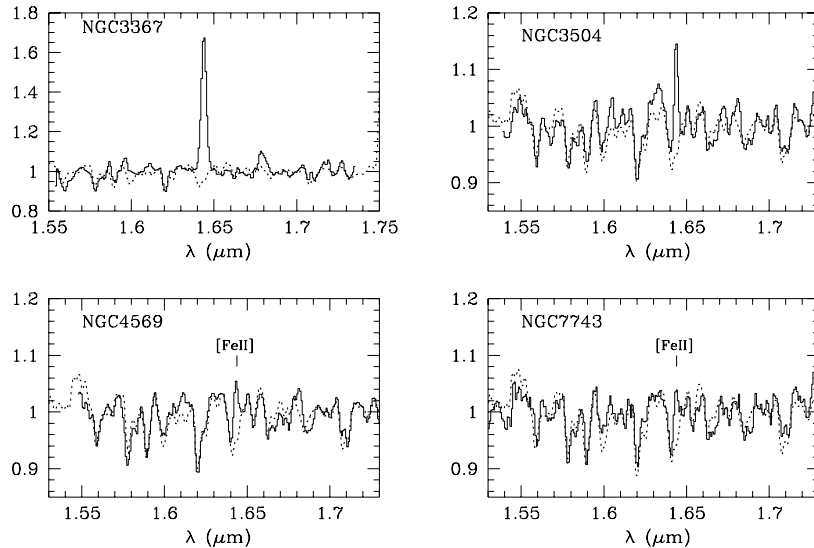


FIG. 4.— Observed H -band spectra of four LINERs (solid line) normalized to unity extracted with a $1.2'' \times 2''$ aperture. For each galaxy we plot as dotted lines the stellar template (composed of M-type supergiants) diluted by a small factor (see text for details).

ing to spectra extracted with a $1.2'' \times 2''$ aperture. Due to the low signal-to-noise of the spectrum of NGC 7743, we did not perform stellar continuum subtraction for it. We used its own off-nucleus spectrum only as the template for NGC 3031. The resulting continuum-subtracted spectra are very flat with most of the absorption features successfully removed, suggesting that the template matches quite well the underlying stellar emission of LINERs. The removal of the underlying stellar continuum allows the detection of weak emission lines. From Figure 3, it can be seen that now $\text{Pa}\beta$ appears in emission in all the galaxies, except NGC 2639 and NGC 4579, where the detection is only marginal. For NGC 3367 and NGC 3504, we also detect additional lines at rest wavelengths (marked in Figure 3): $\lambda = 1.296 \pm 0.001 \mu\text{m}$ (possible identifications $[\text{Fe II}]1.2943 \mu\text{m}$ and $\text{He I}\lambda 1.2968 \mu\text{m}$), $\lambda = 1.311 \pm 0.001 \mu\text{m}$ ($\text{H}_2(4,2)\text{S}(1)\lambda 1.3112 \mu\text{m}$) and $\lambda = 1.321 \pm 0.001 \mu\text{m}$ ($[\text{Fe II}]1.3205 \mu\text{m}$). These lines are also reported in the starburst galaxy M82 (McLeod et al. 1993).

In Table 5 we give the $[\text{Fe II}]1.257 \mu\text{m}/\text{Pa}\beta$ line ratios for large apertures (typically the apertures used to flux-calibrate the data, except for NGC 3998 where we used a $1.2'' \times 4''$ aperture), small apertures ($1.2'' \times 2''$), and that measured from the continuum subtracted spectra. We also compare the continuum-subtracted $\text{Pa}\beta$ fluxes with the $\text{Pa}\beta$ fluxes predicted from $\text{H}\alpha$ fluxes (not corrected for absorption) measured through apertures of similar area to that given in column (7) of Table 5. In general the agreement between the measured $\text{Pa}\beta$ fluxes and those predicted from the optical data is reasonably good.

A similar procedure was applied to the H -band spectra (calibrated spectra are presented in Figure 4, solid lines), but in this case we synthesized the normal galaxy spectrum using an H -band stellar library (Engelbracht, private communication). As for the J -band data, before the stellar continuum subtraction, the galaxy spectra were shifted to rest frame wavelength, and the continuum normalized to unity. We subtracted different empirical stellar templates (composed of different spectral types and luminosities) and found that the best result for all galaxies was obtained with a combination of M supergiants. However, the stellar features had to be diluted to fit the galaxy absorption features. The dilution factors used for each galaxy are: 0.5 for NGC 3367 and NGC 4569, and 0.7 for NGC 3504 and NGC 4569. The stellar templates are plotted for each galaxy as dotted lines in Figure 4. It is likely that the spectra are dominated by AGB stars and perhaps by relatively low mass supergiants; the dilution of the composite supergiant spectrum is an *ad hoc* way to achieve a good fit, until a true population synthesis can be performed. The stellar continuum subtracted spectra of NGC 3367, NGC 3504, NGC 4569 and NGC 7743 in H are presented in Figure 5a (intermediate resolution), whereas in Figure 5b we plot the high resolution spectra of NGC 3504 together with the stellar continuum subtracted data. Again the spectra in Figures 5a and 5b correspond to the spectra extracted with a $1.2'' \times 2''$; from these two figures it can be seen that most of the absorption features have been successfully removed. Note in Figure 4 the presence of a strong CO absorption feature near the $[\text{Fe II}]1.644 \mu\text{m}$ emission line,

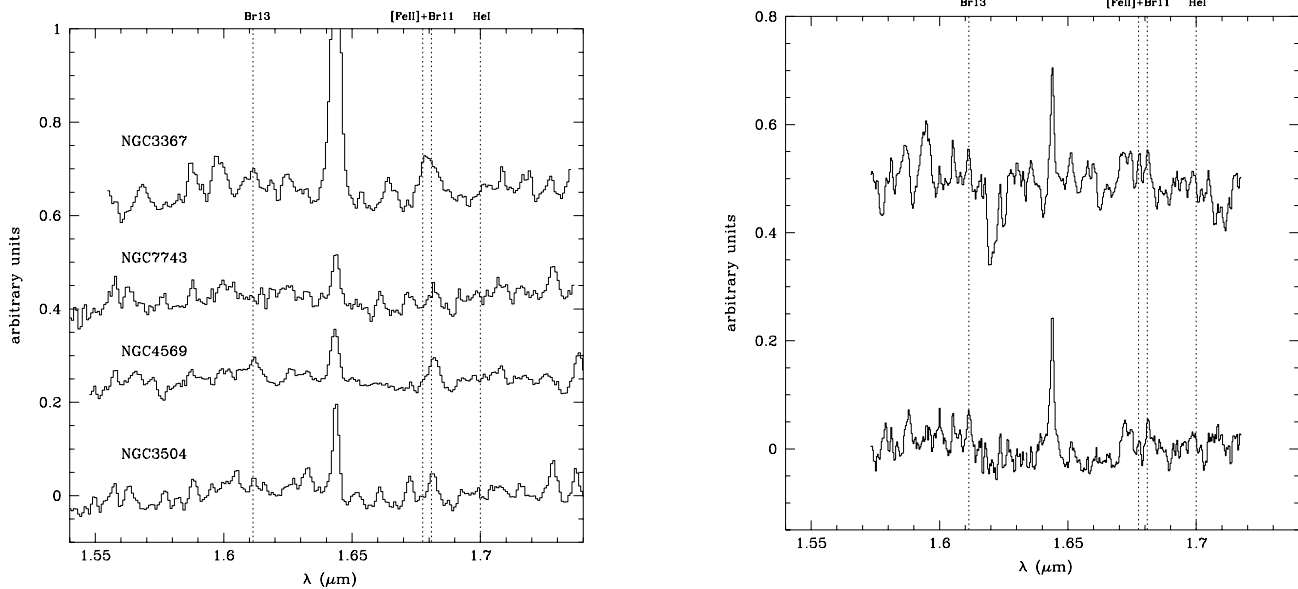


FIG. 5.— *Left panel.* Stellar continuum subtracted spectra in the H -band shifted to rest frame wavelength. The spectra have been shifted vertically by arbitrary amounts for displaying purposes. We mark the expected positions of the emission lines Br13, $[\text{Fe II}]1.677 \mu\text{m}$, Br11 and $\text{He I}1.70 \mu\text{m}$. Br11 is observed blended with $[\text{Fe II}]1.677 \mu\text{m}$ in the intermediate resolution spectra, whereas both lines are clearly separated in the high resolution spectrum of NGC 3504. The He I is not clearly detected. *Right panel.* Observed high resolution spectra (top) at $1.63 \mu\text{m}$ and $1.68 \mu\text{m}$ of NGC 3504, and stellar continuum subtracted spectra (bottom).

which effectively dilutes the latter line in NGC 4569 and NGC 7743. In Figure 5a we see how the $[\text{Fe II}]$ line, barely seen in NGC 4569 and NGC 7743 (Figure 4), is recovered in the stellar continuum subtracted spectra.

The $\text{He I}(1.70 \mu\text{m})/\text{Br}10$ line ratio is very sensitive to the stellar temperature and almost reddening and electron temperature independent, and it is found to be $\text{He I}/\text{Br}10 \simeq 0.35$ for stellar temperatures of 40,000 K (Vanzi et al. 1996). The main purpose of the continuum subtraction in the H -band is to detect (or set an upper limit) to the fluxes of Br11 (and Br10) and $\text{He I} 1.70 \mu\text{m}$. To help with the identifications, we mark the vacuum wavelengths of Br13, Br11, $[\text{Fe II}]1.677 \mu\text{m}$ and $\text{He I} 1.70 \mu\text{m}$ in Figures 5a and 5b. In the intermediate resolution data, the Br11 line appears to be blended with the $[\text{Fe II}]1.677 \mu\text{m}$ line, whereas the He I is not detected. The high resolution spectra of NGC 3504 show the Br11 and $[\text{Fe II}]1.677 \mu\text{m}$ resolved (Figure 5b). In Table 6 we give the flux, equivalent width and FWHM (corrected for the instrument resolution) of the $[\text{Fe II}]1.644 \mu\text{m} + \text{Br}12$ lines, together with the predicted fluxes for the Br11 and Br12 lines from the observed values of $\text{Pa}\beta$ (and from $\text{Br}\gamma$ when available). The last column gives the line ratio $[\text{Fe II}]1.257 \mu\text{m}/[\text{Fe II}]1.644 \mu\text{m}$ for the four galaxies as measured from stellar continuum subtracted spectra; the theoretical value for this line ratio is 1.36 and is independent of the physical conditions (Nussbaumer & Storey 1988). The Br11 (at $1.681 \mu\text{m}$) line fluxes for NGC 3504 and NGC 3367 are measured from the stellar-continuum subtracted spectra, and converted into Br10 fluxes using the theoretical line ratio $\text{Br}10/\text{Br}11 = 1.33$ (Hummer & Storey 1987). Our upper limit to the line flux of the He I line leads to $\text{He I}/\text{Br}10 < 0.26$ in both NGC 3504 and NGC 3367 and places an upper limit of $\simeq 40,000 \text{ K}$ on the

stellar temperature.

3.2. LINER Classification from the $[\text{Fe II}]1.257 \mu\text{m}/\text{Pa}\beta$ line ratio

The $[\text{Fe II}]1.257 \mu\text{m}/\text{Pa}\beta$ (or $[\text{Fe II}]1.644 \mu\text{m}/\text{Br}\gamma$) line ratio used in conjunction with $[\text{O I}]\lambda 6300/\text{H}\alpha$ has proven to be useful in separating different types of activity (Mouri et al. 1990; Goodrich, Veilleux, & Hill 1994; Simpson et al. 1996; Alonso-Herrero et al. 1997; Veilleux, Goodrich, & Hill, 1997). In Alonso-Herrero et al. (1997) we showed that the behavior of both the near-infrared and the optical line ratios can be understood as a progression in the proportion of shock excitation going from H II regions, through starbursts and Seyferts to SNRs. In Figure 6 we show an $[\text{Fe II}]1.257 \mu\text{m}/\text{Pa}\beta$ vs. $[\text{O I}]\lambda 6300/\text{H}\alpha$ diagram where we plot data for our sample of LINERs, together with the line ratios of NGC 1052 and NGC 253. In addition we show Larkin et al.'s (1998) sample of LINERs as filled squares, which represent the near-IR line ratio obtained by them from the $\text{Pa}\beta$ flux predicted from $\text{H}\alpha$. The boxes indicate the approximate locations of starburst and Seyfert galaxies.

From the same type of diagram Larkin et al. (1998) concluded that there are two classes of LINERs, weak- $[\text{Fe II}]$ LINERs ($[\text{Fe II}]1.257 \mu\text{m}/\text{Pa}\beta < 2$) and strong- $[\text{Fe II}]$ LINERs ($[\text{Fe II}]1.257 \mu\text{m}/\text{Pa}\beta > 2$); according to these authors the former class would be low luminosity AGNs, whereas the latter class of LINERs would be powered by starbursts. However, we could easily reach the opposite conclusion. Four objects in our sample appear to be (or have been) dominated by star formation, NGC 3504 (Alonso-Herrero et al. 1997 and references therein), NGC 253 (Engelbracht et al. 1998), NGC 3367 (there is evidence for the presence of Wolf-Rayet stars, Ho et al. 1995), and

TABLE 5
 $[\text{Fe II}]1.257 \mu\text{m}/\text{Pa}\beta$ LINE RATIOS AND $\text{Pa}\beta$ FLUXES.

Galaxy (1)	large (2)	$[\text{Fe II}]/\text{Pa}\beta$ small (3)	subtracted (4)	measured (5)	$f(\text{Pa}\beta)$ predicted (6)	Optical Aperture (7)
NGC 2639	> 6.9	> 7.8	13.0 ± 1	1.10×10^{-15}	2.36×10^{-15}	$1'' \times 4''$
NGC 3031	> 2.7	> 3.0	1.50 ± 0.50	1.80×10^{-14}	1.14×10^{-14}	$1'' \times 4''$
NGC 3367	0.61	0.59	0.58 ± 0.05	2.21×10^{-14}	1.16×10^{-14}	?
NGC 3504	0.47	0.60	0.54 ± 0.05	5.20×10^{-14}	1.89×10^{-14}	$1'' \times 4''$
NGC 3998	> 4.0	> 3.5	3.45 ± 0.30	4.10×10^{-15}	6.25×10^{-15}	$1'' \times 4''$
NGC 4569	2.4	3.5	1.50 ± 0.40	1.13×10^{-14}	2.08×10^{-14}	round $2''$
NGC 4579	> 3.2	> 4.0	3.30 ± 0.30	3.60×10^{-15}	2.78×10^{-15}	round $2''$
NGC 5953	1.40	2.20	1.90 ± 0.20	5.80×10^{-15}	1.02×10^{-14}	?
NGC 7743	...	> 6.3	...	$< 9 \times 10^{-16}$	2.64×10^{-15}	$2'' \times 4''$

NOTE.—Col. (1) Galaxy. Col. (2)–(4) $[\text{Fe II}]1.257 \mu\text{m}/\text{Pa}\beta$ line ratio measured from the spectra extracted with the large and small aperture, and from the stellar continuum subtracted spectrum (small aperture). Col. (5) $\text{Pa}\beta$ line fluxes (in $\text{erg cm}^{-2} \text{s}^{-1}$) measured from the stellar continuum subtracted spectra with apertures similar to optical spectroscopy, column (7). When the optical aperture is not given, the $\text{Pa}\beta$ flux corresponds to the $1.2'' \times 2''$ aperture. Col. (6) $\text{Pa}\beta$ line fluxes (in $\text{erg cm}^{-2} \text{s}^{-1}$) predicted from the $\text{H}\alpha$ fluxes. Col. (7) aperture for data in Col. (5) and (6).

TABLE 6
 H -BAND SPECTRAL FEATURES.

Galaxy (1)	Aperture (2)	$[\text{Fe II}]1.644+\text{Br}12$ flux (3)	EW (4)	FWHM (5)	$f(\text{Br}12)_{\text{pred}}$ (6)	$f(\text{Br}11)_{\text{pred}}$ (7)	Ratio $[\text{Fe II}]$ $1.257/1.644$ (8)
NGC 3367	$1.2'' \times 6''$	1.19×10^{-14}	19.2	< 400	6.8×10^{-16}	8.8×10^{-16}	1.1
	$1.2'' \times 2''$	9.34×10^{-15}	23.0	< 400
NGC 3504	$1.2'' \times 8.5''$	2.45×10^{-14}	4.7	< 400	2.6×10^{-15}	3.4×10^{-15}	1.7
	$1.2'' \times 2''$	1.05×10^{-14}	4.1	< 400
	$1.2'' \times 2''^{\text{a}}$	2.30×10^{-14}	3.8	200	...	$5.1 \times 10^{-15\text{b}}$...
NGC 4569	$1.2'' \times 8.5''$	1.40×10^{-14}	1.5	< 400	2.2×10^{-16}	2.9×10^{-16}	1.2
	$1.2'' \times 2''$	6.84×10^{-15}	1.2	< 400
NGC 7743	$1.2'' \times 6''$	$< 4.3 \times 10^{-15}$	2.9×10^{-17}	3.8×10^{-17}	1.3

NOTE.—Col. (1) Galaxy. Col. (2) Extraction aperture. Col. (3) Flux in $\text{erg cm}^{-2} \text{s}^{-1}$. Col. (4) EW in \AA . Col. (5) FWHM in km s^{-1} (corrected for instrumental resolution). Col. (6) Flux of Br12 ($\text{erg cm}^{-2} \text{s}^{-1}$) computed from $\text{Pa}\beta$. Col. (7) Flux of Br11 ($\text{erg cm}^{-2} \text{s}^{-1}$) computed from $\text{Pa}\beta$. Col. (8) $[\text{Fe II}]1.257 \mu\text{m}/[\text{Fe II}]1.644 \mu\text{m}$ line ratio.

^aHigh-resolution data

^bMeasured

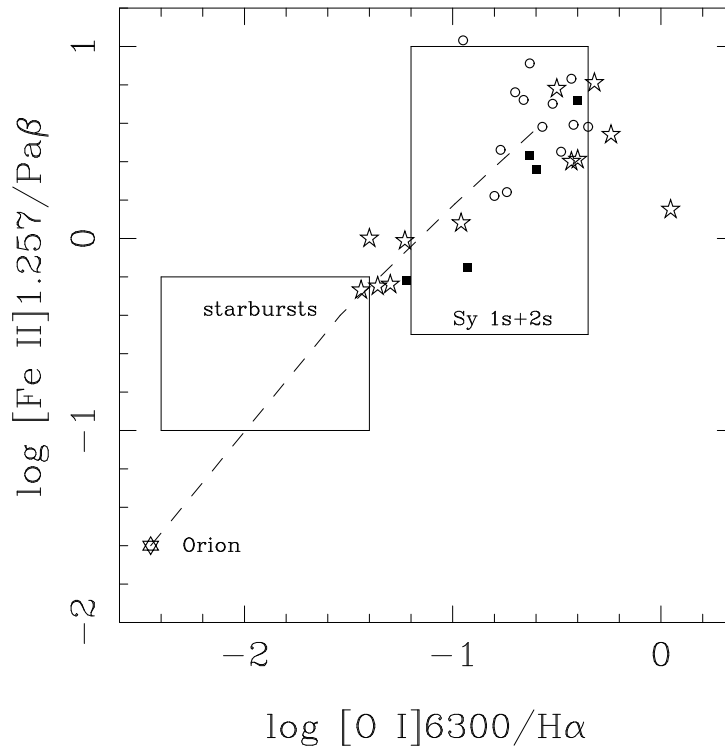


FIG. 6.— $[\text{Fe II}]1.257 \mu\text{m}/\text{Pa}\beta$ vs. $[\text{O I}]\lambda 6300/\text{H}\alpha$ diagram. The star symbols are our sample of galaxies (including NGC 1052 and NGC 253), the filled squares are Larkin et al. (1998) LINERs. The open circles are SNRs from Lumsden & Puxley (1995). The dashed line represents a mixing curve of a pure H II region (e.g., Orion) and SNRs. The boxes indicate the approximate location of the regions occupied by starbursts and Seyfert galaxies.

NGC 4569 (Keel 1996; Maoz et al. 1998); all these objects show $[\text{Fe II}]1.257 \mu\text{m}/\text{Pa}\beta < 0.70$, and can be classified as weak-[O I] LINERs. Another group of LINERs shows evidence for having an AGN, mainly based on the detection of a broad component in $\text{H}\alpha$: NGC 3031 (Filippenko & Sargent 1988), NGC 2639 and NGC 3998 (Filippenko & Sargent 1985), and NGC 4579 (Ho et al. 1995). All these galaxies have $[\text{Fe II}]1.257 \mu\text{m}/\text{Pa}\beta > 1.40$. If now we turn to Larkin et al. (1998) sample, we find that NGC 404 and NGC 4736 may have had recent star formation (Maoz et al. 1998; Ho et al. 1993, 1995, and Walker et al. 1988 and Taniguchi et al. 1996 respectively), yet $[\text{Fe II}]1.257 \mu\text{m}/\text{Pa}\beta > 3$. NGC 4258 has broad $\text{H}\alpha$ (Filippenko & Sargent 1985), and NGC 5194 is classified as intermediate between LINER and Seyfert; both have $[\text{Fe II}]1.257 \mu\text{m}/\text{Pa}\beta = 0.6 - 2$. NGC 4826 has optical line ratios (Keel 1983) which locate it in the LINER region in diagnostic diagrams (Veilleux & Osterbrock 1987; Ho et al. 1997a), but it is a weak-[O I] LINER with $[\text{Fe II}]1.257 \mu\text{m}/\text{Pa}\beta = 0.7$. Distinguishing different types of LINERs solely from the $[\text{Fe II}]1.257 \mu\text{m}/\text{Pa}\beta$ ratio appears to be problematic.

3.3. LINERs powered by an evolved starburst

Although AGN excitation can be identified in some LINERs through the detection of a broad component of $\text{H}\alpha$, we believe many other LINERs are powered by an aging starburst. We find candidates for the latter category among weak-[O I] LINERs and starburst/LINER transition objects as well as some *pure* LINERs (i.e., those which satisfy the Heckman (1980) LINER definition).

The emission-line behavior of starbursts can be understood as a transition from pure H II region in the first ~ 10 million years, to an increasing role of shock excitation by supernova remnants, possibly ending with a pure supernova-like shock excited spectrum (Rieke et al. 1993; Genzel et al. 1995; Engelbracht et al. 1996, 1998; Böker, Förster-Schreiber, & Genzel 1997; Vanzi et al. 1998). This transition occurs because the hot, ionizing stars in a starburst stellar population have lifetimes of only a few million years, while supernovae are produced by stars that are of relatively low mass and are only relatively weak UV emitters (see, e.g., the starburst models of Leitherer & Heckman 1995).

We propose that traditional weak-[O I] LINERs and H II/LINERs arise as the episode of star formation ages and the SNRs start making an important contribution to the observed flux of the [Fe II] lines, as well as to the low-ionization optical emission lines. The $[\text{Fe II}]1.257 \mu\text{m}/\text{Pa}\beta$ line ratio will rise as the number of SNR increases and the ionization flux from very young stars decreases (and therefore the $\text{Pa}\beta$ flux). This hypothesis has been proven to be successful in explaining the transitional LINER/H II line ratios of NGC 253 (Engelbracht et al. 1998).

Simpson et al. (1996) advanced the idea that the $[\text{Fe II}]1.257 \mu\text{m}/\text{Pa}\beta$ line ratio could be used as an indicator of the age of the starburst. Colina (1993) set an upper limit to the $[\text{Fe II}]1.644 \mu\text{m}/\text{Br}\gamma$ line ratio (1.42 or $[\text{Fe II}]1.257 \mu\text{m}/\text{Pa}\beta = 0.33$) produced by star formation processes. However, Vanzi & Rieke (1997) calibrated the [Fe II] emission in terms of the SN rate by means of M82, and showed that when this relationship is combined with

an evolutionary synthesis model one can reproduce a variety of $[\text{Fe II}]1.644 \mu\text{m}/\text{Br}\gamma$ line ratios from $\simeq 2 \times 10^{-3}$ for very young starbursts up to 10 for evolved starbursts. The latter ratio is considerably higher than the upper limit imposed by Colina's (1993) models. In Figure 7 we present a plot of $[\text{Fe II}]1.644 \mu\text{m}/\text{Br}\gamma$ versus $\log(K/\text{Br}\gamma)$. The latter quantity is proportional to the inverse of the equivalent width of $\text{Br}\gamma$ and is expressed in units of μm^{-1} . We show in this diagram the LINERs believed to be dominated by star formation from our sample and other references as filled squares and star-like symbols respectively. The AGN-dominated LINERs are plotted as open circles. Also displayed in this figure is a starburst model (Rieke et al. 1993) with burst duration of 1 Myr (FWHM) (see figure caption for a detailed explanation). For the LINERs the $\text{Br}\gamma$ fluxes are derived from the $\text{Pa}\beta$ fluxes using the theoretical value given in Hummer & Storey (1987), whereas the $\text{Br}\gamma$ equivalent width is estimated from the $\text{Pa}\beta$ equivalent width and assuming a color $J - K = 1$ (which is almost independent of the stellar population). This figure shows that both the $[\text{Fe II}]1.644 \mu\text{m}/\text{Br}\gamma$ line ratio and $K/\text{Br}\gamma$ can be used to constrain the age of the burst in those cases in which the LINER activity is dominated by star formation. We find that the weak-[O I] LINERs NGC 253, NGC 3367, NGC 3504, NGC 4569 and NGC 4826 have burst ages (defined as the time elapsed after the peak of star formation) between 8 and 11 Myr, whereas the classical LINERs NGC 404 and NGC 4736 seem to be in a more advanced stage, with burst ages > 12 Myr. The LINER/Wolf-Rayet galaxy NGC 6764 has an age $\simeq 9 - 10$ Myr. This model would only work if the burst duration is short compared with to the evolutionary lifetimes of massive stars as in the case of the 1 Myr burst.

The idea that some LINERs are powered by stars is not new; for instance Filippenko & Terlevich (1992) and Shields (1992) proposed that the optical line ratios of LINERs can be explained in terms of photoionization by hot stars ($\geq 45,000$ K) in a dense medium. However more recently, Engelbracht et al. (1998) derived an upper limit of 37,000 K on the stars exciting the emission lines in the weak-[O I] LINER/H II galaxy NGC 253, based on different arguments. One of those arguments involves the observed value of the $\text{He I}(1.70 \mu\text{m})/\text{Br}10 (< 0.25)$ line ratio, which is predicted to be around 0.35 for hot stars ($T > 40,000$ K). For two galaxies in our sample, NGC 3367 and NGC 3504, we set the same upper limit for the stellar temperature (Section 3.1). The second argument used by Engelbracht et al. (1998) is that hot stars are not needed to reproduce the optical line ratios of NGC 253. These authors assume that all the $[\text{Fe II}]$ line emission is produced by supernovae (Vanzi & Rieke 1997 and references therein), and use photoionization models for metal-rich H II regions (Shields & Kennicutt 1995) to predict the line ratios for photoionized gas. Combining the two excitation mechanisms produced a satisfactory fit to the overall spectrum of the galaxy. In this fit, supernovae contribute a significant portion of optical lines such as $[\text{O III}]\lambda 5007$, $[\text{O I}]\lambda 6300$ and $[\text{S II}]\lambda\lambda 6713, 6731$.

We will take a similar approach to try and reproduce the line ratios of those LINERs without evidence for an AGN. We determine the $[\text{Fe II}]1.257 \mu\text{m}/\text{Pa}\beta$ line ratios for the supernovae together with the $[\text{O I}]\lambda 6300$ and $[\text{S II}]\lambda\lambda 6713, 6731$ from the study of Lumsden & Puxley

(1995), which allows us to obtain average values for the $[\text{O I}]\lambda 6300/[\text{Fe II}]1.257 \mu\text{m}$ and $[\text{S II}]/[\text{Fe II}]1.257 \mu\text{m}$ line ratios. The data for the $[\text{O III}]\lambda 5007$ and $[\text{N II}]\lambda 6583$ lines are from Smith et al. (1993) and Blair & Kirshner (1985). All these lines are ratioed to $[\text{Fe II}]1.257 \mu\text{m}$ through hydrogen recombination lines, assuming Case B line ratios for the latter lines. To represent the H II region component we use the models presented in Shields & Kennicutt (1995). We choose models with solar metallicity, including dust effects, and photoionized by a single star with four different temperatures: $T = 35,000, 38,000, 42,000$ and $45,000$ K (calculated as described in Shields & Kennicutt 1995 using CLOUDY 90.03). For each galaxy, we use the $[\text{Fe II}]1.257 \mu\text{m}/\text{Pa}\beta$ line ratio to set the contribution of SNRs to the observed optical line ratios. In Figure 8 we display mixing curves of an H II region component with the different stellar temperatures and the SNR component. The symbols on the lines indicate $[\text{Fe II}]1.257 \mu\text{m}/\text{Pa}\beta$ line ratios from left to right of 0. (that is, pure H II region), 0.5, 1, 2, 3, 4, 5, and 6. The starburst-dominated LINERs are plotted as filled circles, whereas the AGN-dominated LINERs are plotted as open circles. From these diagrams (see also Table 7) we observe that the mixed model with stellar temperature $T = 38,000$ K provides a reasonable fit to almost all the potentially starburst-dominated LINERs.

As an illustration of the calculations, we present in Table 7 the line ratios both observed and predicted by the model with stellar temperature $T = 38,000$ K for all the galaxies with evidence for star-formation. Two basic assumptions are used in this calculation. First we are taking average line ratios for SNRs, while an age effect could be present, that is, more evolved SNRs show slightly different average line ratios. Second, we are representing the H II region component as photoionized by stars with a single temperature. This may be true for the intermediate age starburst LINERs, but for the most evolved starburst LINERs this may not be a good representation. For instance for ages > 5 Myr the $[\text{N II}]\lambda 6583/\text{H}\alpha$, $[\text{O I}]\lambda 6300/\text{H}\alpha$ and $[\text{S II}]\lambda\lambda 6713, 6731/\text{H}\alpha$ ratios slightly increase as the starburst evolves, whereas the $[\text{O III}]\lambda 5007/\text{H}\beta$ ratio decreases rapidly as the number of hot stars drops (see for example the models of García-Vargas, Bressan, & Díaz 1995, and Stasińska & Leitherer 1996). This last ratio is however easily maintained with the presence of SNRs.

In all cases but NGC 6764 the observed line ratios were measured from stellar continuum subtracted spectra (see references in the notes of the table). The range of observed line ratios corresponds to different references, and gives an idea of the uncertainties associated with these numbers. The errors associated with the line ratios predicted by our H II-SNR models are simply the propagation of the errors in the measured $[\text{Fe II}]1.257 \mu\text{m}/\text{Pa}\beta$ line ratio. A 10% error in the determination of the $[\text{Fe II}]1.257 \mu\text{m}/\text{Pa}\beta$ line ratio would lead to errors in the model predictions of about 10% in the $[\text{O III}]\lambda 5007/\text{H}\beta$ line ratio, 1% in $[\text{N II}]\lambda 6583/\text{H}\alpha$, 10% in $[\text{O I}]\lambda 6300/\text{H}\alpha$ and 5% in $[\text{S II}]\lambda\lambda 6713, 6731/\text{H}\alpha$. The shock excitation produced by the SNRs accounts for between 72% and 100% of the $[\text{O I}]\lambda 6300$ line, between 25% and 80% of the $[\text{S II}]\lambda\lambda 6713, 6731$ lines, between 6% and 44% of the $[\text{N II}]\lambda 6583$ line, and between 42% and 69% of the $[\text{O III}]\lambda 5007$ line in the LINERs analyzed here.

From Table 7 we find that there is a very good agree-

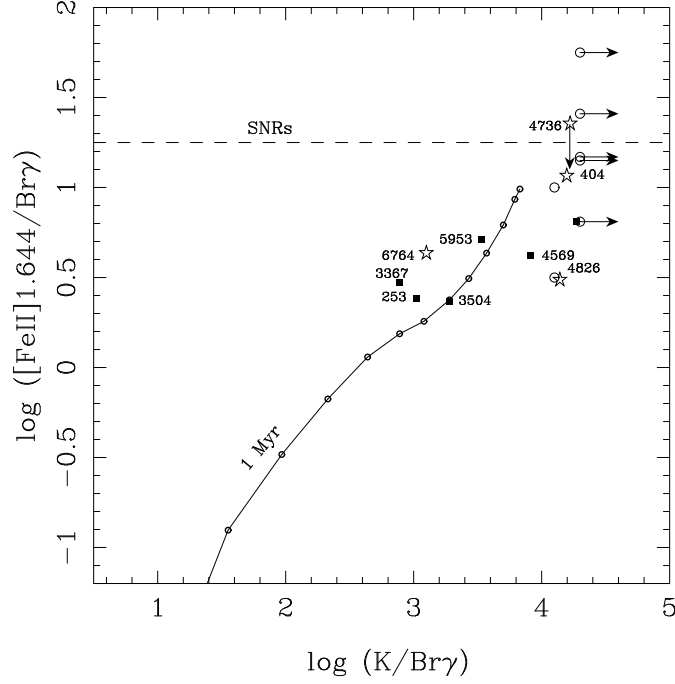


FIG. 7.— $[\text{Fe II}]1.644 \mu\text{m}/\text{Br}\gamma$ vs. $\log(K/\text{Br}\gamma)$ diagram. The units for $\log(K/\text{Br}\gamma)$ are μm^{-1} . The solid line is the output of a starburst model (Rieke et al. 1993) with the $[\text{Fe II}]$ calibration described in Vanzi & Rieke (1997) for a Gaussian burst of duration 1 Myr (FWHM). For this curve the points are spaced 1 Myr, and the first point on the curve (to the left) represents 2 Myr after the peak of star formation. The filled squares (our sample) and star-like symbols (Calzetti 1997 and Larkin et al. 1998) are starburst-dominated LINERs. The open circles are AGN-dominated LINERs. The dashed line represents the average $[\text{Fe II}]1.644 \mu\text{m}/\text{Br}\gamma$ line ratio for SNRs.

TABLE 7

OBSERVED LINE RATIOS, AND MODEL PREDICTIONS ($T_* = 38,000 \text{ K} + \text{SNR}$) FOR THE STARBURST-DOMINATED LINERs.

Galaxy	$[\text{O III}]5007/\text{H}\beta$	$[\text{O I}]6300/\text{H}\alpha$	$[\text{N II}]6583/\text{H}\alpha$	$[\text{S II}]6713,6731/\text{H}\alpha$	$[\text{Fe II}]/\text{Pa}\beta$
NGC 253	0.47	0.044	0.78	0.40	0.56 ± 0.05
model	0.55 ± 0.03	0.053 ± 0.003	0.78 ± 0.01	0.47 ± 0.01	
NGC 404	1.29 – 1.78	0.17 – 0.23	0.44 – 0.57	0.94 – 1.03	2.70
model	1.73	0.21	1.03	1.03	
NGC 3367	0.50	0.031 – 0.050	0.83 – 0.87	0.28 – 0.37	0.58 ± 0.05
model	0.56 ± 0.03	0.055 ± 0.003	0.79 ± 0.01	0.48 ± 0.01	
NGC 3504	0.53 – 0.63	0.023 – 0.036	0.59 – 0.65	0.28	0.54 ± 0.05
model	0.53 ± 0.03	0.050 ± 0.003	0.78 ± 0.01	0.46 ± 0.01	
NGC 4569	0.72 ^a –1.18	0.062 – 0.081	0.90	0.40 – 0.50	1.50 ± 0.5
model	1.05 ± 0.26	0.12 ± 0.035	0.89 ± 0.06	0.72 ± 0.13	
NGC 4736	1.47–2.48 ^a	0.24 – 0.40	2.15 – 3.61	1.39 – 2.49	5.30
model	3.17	0.41	2.35	1.98	
NGC 4826	0.50 – 1.45	0.073 – 0.12	0.82 – 1.27	0.64 – 0.77	0.70
model	0.63	0.07	0.80	0.55	
NGC 6764	0.58	0.040 – 0.065	0.68 – 0.75	0.29 – 0.46	1.0 ± 0.2
model	0.79 ± 0.10	0.087 ± 0.015	0.83 ± 0.02	0.59 ± 0.05	

^a $\text{H}\beta$ flux derived from $\text{H}\alpha$, assuming $\text{H}\alpha/\text{H}\beta = 2.70$.

NOTE.—References for the optical line ratios are as follows, NGC 253 Armus, Heckman, & Miley (1989), and Tadhunter et al. (1993); NGC 404 Keel (1983), Ho et al. (1993, 1997a); NGC 4736 and NGC 4826 Keel (1983) and Ho et al. (1997a); NGC 6764 Eckart et al. (1996).

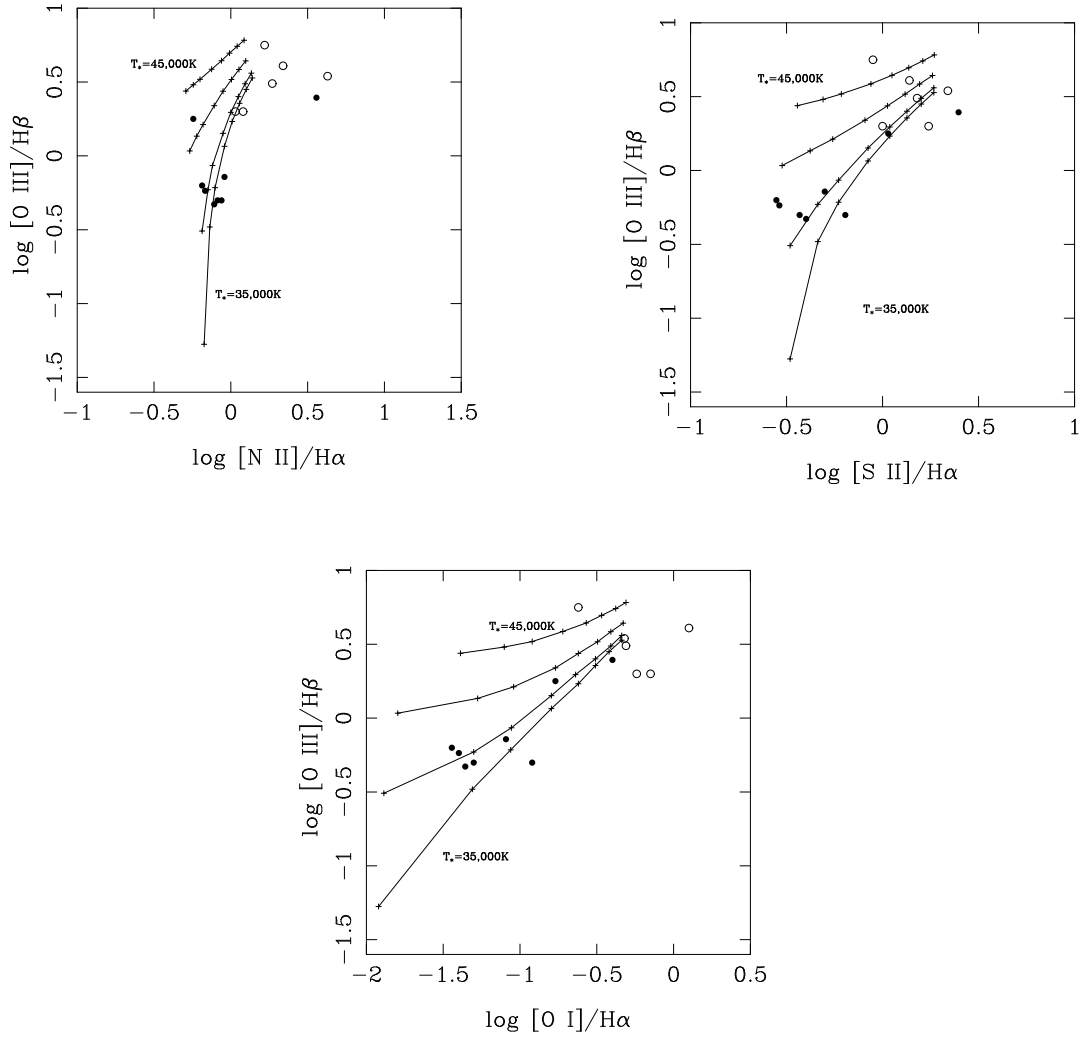


FIG. 8.— Line ratio diagrams where the mixing curves of H II region model with temperatures $T = 35,000, 38,000, 42,000$ and $45,000$ K and SNR are plotted as solid lines. The filled circles are the optical line ratios of those starburst-dominated LINERs, whereas the open circles are line ratios of the AGN-dominated LINERs. The symbols on the curves indicate indicate $[Fe II]1.257 \mu m/Pa\beta$ line ratios from left to right of 0. (that is, pure H II region), 0.5, 1, 2, 3, 4, 5, and 6.

ment between the observed and the predicted ratios for NGC 253, NGC 3367 and NGC 4569, and reasonably good correspondence for NGC 404, NGC 3504, NGC 4736 and NGC 4826. NGC 6764 shows optical line ratios very similar to those of NGC 3504, however its [Fe II]1.257 $\mu\text{m}/\text{Pa}\beta$ line ratio is twice as large; one reason for the discrepancy of the predicted line ratios could be the difference in aperture size between the optical and the near-infrared line ratios. The largest discrepancies seem to occur for the [S II] $\lambda\lambda 6713, 6731/\text{H}\alpha$ line ratio, the model always giving an overproduction of [S II]. However, the average [S II] $\lambda\lambda 6713, 6731/[\text{Fe II}]1.257 \mu\text{m}$ ratio derived for SNRs is quite uncertain since this line ratio ranges from 2.87 to 10.52 (Lumsden & Puxley 1995), making the predicted ratios uncertain by a factor of two.

Despite the fact that our fitting technique is not very sophisticated, it provides a very plausible fit to the line ratios in most of the weak-[O I]6300 and some classical LINERs. A separate set of calculations confirms that we can account for the line ratios in many of these galaxies with very hot ($T > 45,000\text{K}$) stars as was pointed out by Filippenko & Terlevich (1992). Thus, neither set of fits is unique for starburst-dominated LINERs, and the choice between them depends on other evidence. In this regard, the upper limits of 40,000K for the stellar temperature we have set for NGC 3504 and NGC 3367 would indicate that the new class of fit is to be preferred. Second, the high-stellar-temperature models have trouble reproducing cases with strong [O III] as well as low-ionization lines, such as those toward the upper right in Figure 8.

Very hot stars appear to dominate starbursts for very short times. Therefore, we believe that the success of the lower temperature/shock excitation model is strong evidence that many LINERs are aging starbursts, in which the SNRs play an increasingly important role as the starburst ages. Not all the LINERs studied in this paper fall into either of these categories though. NGC 2639, NGC 1052, NGC 3031, NGC 3998, NGC 4579 and NGC 7743 have optical line ratios which are not easily modeled with the composite H II region – SNR model. Although we do not rule out the possibility that star formation is playing some role, it seems that in this group of objects the low-luminosity AGN is dominant.

4. TEST OF THE LINER-STARBURST CONNECTION

4.1. General Behavior

We can explore the LINER-Starburst connection through a simple parameterization of the behavior of a starburst galaxy. We take a typical mass-luminosity relation:

$$L(M) = K M^\alpha \quad (1)$$

where M is the stellar mass and L its luminosity (and K a constant). α is $\simeq 3$ for stars with $M > 10 M_\odot$ (Vacca, Garmany, & Shull 1996). We approximate the main sequence lifetime of a star as,

$$T_{\text{ms}} \propto \frac{M}{L} \quad (2)$$

Now we assume a starburst in which all stars are formed simultaneously. It can then be shown that the mass at the

main sequence turnoff as a function of the starburst age (t) is approximately:

$$M_{\text{ms}}(t) = K_1 t^{-\frac{1}{\alpha-1}} \quad (3)$$

where K_1 is a constant. We take the initial mass function IMF (for high mass stars) in the starburst to be (with upper mass cutoff M_u):

$$\phi(M) dM = C M^\gamma dM, \quad (4)$$

where C is a constant. With these approximations, the supernova rate (SNr) can be computed as,

$$(\text{SNr}) = \phi(M) \frac{dM_{\text{ms}}}{dt} \propto t^{-\frac{\gamma+\alpha}{\alpha-1}} \quad (5)$$

Using a similar approach, the starburst luminosity is:

$$L_{\text{sb}} = \int_{M_1}^{M_u} \phi(M) L(M) dM \simeq \quad (6)$$

$$\int_{M_1}^{M_{\text{ms}}} \phi(M) L(M) dM \propto M_{\text{ms}}^{\gamma+\alpha+1} \propto t^{-\frac{\gamma+\alpha+1}{\alpha-1}} \quad (7)$$

We have made the approximation that all the luminosity emerges from stars near the main sequence turnoff (M_{ms}) in simplifying the integral. Additional luminosity is produced by stars in post-main-sequence evolution, but it would correct the expression by only a small factor, and since these stages are predominantly at much lower stellar temperature than the main sequence ones, much of this luminosity may escape the starburst region. Thus, from equations [5] and [6] we get that the starburst luminosity to supernova rate ratio does not depend upon the IMF slope, and using the nominal value of α goes as,

$$\frac{L_{\text{sb}}}{(\text{SNr})} \propto t^{\frac{-1}{\alpha-1}} \propto t^{-0.5} \quad (8)$$

That is, so long as the main sequence turnoff is high enough that virtually all evolving stars end their lives as supernovae (nominally corresponding to a turnoff mass near $8 M_\odot$), then the proportionality between luminosity and supernova rate should change only slightly as the starburst ages.

However, because starburst galaxies are usually identified by their emission lines, it would be more appropriate to use the ionizing luminosity to represent the starburst phase. The ionizing luminosity can be expressed as $L_{\text{ion}} \propto M^\beta$, and in this case, equation [7] becomes,

$$\frac{L_{\text{ion}}}{(\text{SNr})} \propto t^{\frac{\alpha-\beta-1}{\alpha-1}} \quad (9)$$

The value of β is approximately 7 for dwarf stars with effective temperatures between 32,000 K and 40,000 K (Vacca et al. 1996), so the time dependence is:

$$\frac{L_{\text{ion}}}{(\text{SNr})} \propto t^{-2.5} \quad (10)$$

The analytical prediction given in Equation (9) is in good agreement with the model prediction (Figure 7) in which the line ratio [Fe II]1.644 $\mu\text{m}/\text{Br}\gamma$ drops by more than a factor of a hundred between 1 and 10 Myr.

Thus, the nature of the emission spectrum of a galaxy will change rather abruptly from H II-dominated to shock-dominated (Equation 9). This transition will occur while there is still a substantial luminosity from the starburst (Equation 7). We therefore predict that there will be two general classes of luminous starburst-powered galaxy, dominated respectively by hot stellar and shock excitation. Intermediate cases will arise largely because extended periods of star formation can cause parts of the starburst to be in a young phase while other parts have evolved into the shock-excited phase.

4.2. *The relative numbers of starbursts and starburst-dominated LINERs*

To test these predictions, we need to determine when the supernova rate is high enough (compared with the luminosity of the starburst) that we will start detecting LINER characteristics. Pure starbursts could be defined such that the ratio of ionizing radiation to supernova shock-heating is greater than 1. From Figure 7, for a burst of 1 Myr duration (FWHM), the transition occurs after about 6 Myr, as defined by when the ratio of the predominantly shock excited [Fe II] to the predominantly photo-ionized Br γ lines exceeds one. In fitting starbursts with evolutionary models, it is generally found that strong star formation occurs over a period of 5–10 Myr (e.g., Rieke et al. 1993; Genzel et al. 1995; Engelbracht et al. 1996, 1998; Böker et al. 1997; Vanzi et al. 1998). The lifetime of the LINER phase could be defined when the supernova rate drops by a factor of 10 from its peak value (after 30 to 40 Myr). We choose 30 Myr as the maximum age at which we would be able to detect H α in emission, for at older ages the equivalent width of this line would be $< 0.5 \text{ \AA}$ (e.g., Leitherer & Heckman 1995; Leitherer et al. 1999). The predicted behavior of a starburst is then about 14 Myr of photo-ionization domination, followed by about 30 Myr of shock domination. The expected relative number between (young) starburst and starburst-dominated LINERs (aging starbursts) is simply given by the ratio between the durations of each phase, that is, roughly 1:2.

The distance-limited Palomar spectroscopic survey of nearby galaxies (Ho et al. 1997a,c) can be used to test this prediction. From the sample of 486 galaxies, 206 galaxies are classified as H II nuclei. Approximately 100 galaxies classified as H II nuclei show equivalent widths of H α of less than 10 \AA . Among these galaxies we find that approximately 50 of them show $[\text{O I}]/\text{H}\alpha > 0.040$, whereas from figure 7 in Ho et al. (1997a) the arbitrary line for transition objects has been drawn around $[\text{O I}]/\text{H}\alpha = 0.080$. From Figure 8b we can see that objects with $[\text{O I}]/\text{H}\alpha > 0.040$ have already a significant contribution from SNRs, and could be considered (arbitrarily) as evolved starbursts. In addition, for those objects with small values of $\text{EW}(\text{H}\alpha)$ the [O I] line is weak, and the measurement errors are of the order of 20% or 30% (Ho et al. 1997a). Because of these ambiguities, we exclude the galaxies with very faint H α from the sample, leaving roughly 100 starburst galaxies strong enough that we might expect to detect their counterparts as LINERs. 94 sample members are classified as LINERs and 65 galaxies are classified as transition objects (i.e., in Ho et al. 1997c definition these are composite LINER/H II nuclei). About 20% of all AGN/LINER identifications show broad H α and are presumably powered by

a true AGN. We have subtracted this percentage from the the LINER category to isolate the candidate starburst-dominated LINERs. We also exclude the LINER/Seyferts from the LINER category. We find that the relative number of starbursts to starburst-dominated LINERs in the Ho et al. (1997a) sample is about 1:1.4 which is in satisfactory agreement with the prediction, given the necessarily rough nature of the estimates.

4.3. *Morphological Types*

Starbursts appear preferentially in late type spiral galaxies, while LINER nuclei are found mostly in early type galaxies, including ellipticals and S0s. We have examined this trend in further detail using the sample with very high quality spectra described by Ho et al. (1997b). We consider only the galaxies with pure LINER spectra. If galaxies with indications of an AGN are excluded (broad wings on H α , strong radio or X-ray emission), then we find only one elliptical remains within the sample. The morphological type distribution is centered at about Sa and is not significantly different from that for LINER/Transition galaxies.

Thus, the galaxies that plausibly contain aging starbursts are mostly of spiral type, but are earlier than the bona fide starburst galaxies. An interesting possibility is that the consequences of a strong nuclear starburst are to modify the appearance of a galaxy so that it tends to be classified as of an earlier type than before the burst. This change could result from the exhaustion of interstellar gas in the center and the presence of a luminous population of intermediate population stars with the bulge that increase its prominence. An example is provided by NGC 4736, which is a LINER of type Sab. However, a number of lines of evidence suggest that its circumnuclear stellar population is dominated by the products of an aging starburst (e.g., Walker, Lebofsky, & Rieke 1988; Taniguchi et al. 1996). The tendency of a number early type LINERs [NGC 404 (S0), NGC 4569 (Sab), NGC 5055 (Sbc), and NGC 6500 (Sab)] to have UV spectra dominated by hot, massive stars ($T > 30,900\text{K}$) is further evidence that there is a connection between starbursts and early type LINERs (Maoz et al. 1998).

5. CONCLUSIONS

We have presented J -band ($1.15\text{--}1.35 \mu\text{m}$) spectroscopy of a sample of nine galaxies showing some degree of LINER activity (classical LINERs, weak-[O I] LINERs and transition objects), together with H spectroscopy for some of them. All the LINERs show bright [Fe II]1.2567 μm emission, whereas the Pa β line is only detected in emission in three LINERs (before stellar continuum subtraction). Since the J -band spectra of most LINERs in this work are dominated by a strong stellar continuum, we perform a careful subtraction of this continuum to measure more accurate [Fe II]1.2567 μm /Pa β ratios.

We find that the optical and near-infrared emission lines of a significant percentage of LINERs (those with no evidence for an AGN) can be explained by the presence of an evolved starburst. We model the optical line ratios of these LINERs with a metal-rich H II region model with $T_* = 38,000 \text{ K}$, plus a SNR component. The proportions of the two components are set by the [Fe II]1.2567 μm /Pa β

line ratio, since the [Fe II] line is predominantly excited by SNR-driven shocks and the line Pa β tracks H II regions excited by massive young stars. The proposed LINER-starburst connection is tested by predicting the time dependence of the ionizing luminosity of the starburst to the supernova rate $L_{\text{ion}}/(\text{SNr})$. We predict the relative number of starbursts to starburst-dominated LINERs (aging starbursts). The agreement with the observations is relatively good, supporting our hypothesis that many LINERs are aging starbursts.

We thank the anonymous referee for providing com-

ments which helped to improve the paper. We are grateful to Ana Maria Biscaya and Alice Quillen for assisting us with some of the observations presented in this paper.

During the course of this work AA-H was supported by the National Aeronautics and Space Administration on grant NAG 5-3042 through the University of Arizona. The work was also partially supported by the National Science Foundation under grant AST-95-29190. This research has made use of the NASA/IPAC Extragalactic Database (NED) which is operated by the Jet Propulsion Laboratory, California Institute of Technology, under contract with the National Aeronautics and Space Administration.

REFERENCES

- Alonso-Herrero, A., Rieke, M. J., Rieke, G. H., & Ruiz, M. 1997, *ApJ*, 482, 747
- Armus, L., Heckman, T. M., & Miley, G. K. 1989, *ApJ*, 347, 727
- Balzano, V. A., & Weedman, D. W. 1981, *ApJ*, 243, 756
- Barth, A. J., Ho, L. C., Filippenko, A. V., & Sargent, W. L. 1998, *ApJ*, 496, 133
- Barth, A. J., Filippenko, A. V., & Moran, E. C. 1999, *ApJ*, 515, L61
- Blair, W. P., & Kirshner, R. P. 1985, *ApJ*, 289, 582
- Böker, T., Förster-Schreiber, N. M., & Genzel, R. 1997, *AJ*, 114, 1883
- Bushouse, H. A., Stanford, S. A. 1992, *ApJS*, 79, 213
- Calzetti, D. 1997, *AJ*, 113, 162
- Colina, L. 1993, *ApJ*, 411, 565
- Colina, L., García-Vargas, M. L., González-Delgado, R., Mas-Hesse, J. M., Pérez, E., Alberdi, A., & Krabbe, A. 1997, *ApJ*, 488, 71
- Cui, W., Feldkhun, D., & Braun, R. 1997, *ApJ*, 477, 693
- Decker, H., D'Odorico, S., & Arsenault, R. 1988, *A&A*, 189, 353
- Devereux, N. A., Becklin, E. E., & Scoville, N. 1987, *ApJ*, 312, 529
- Eckart, A., Cameron, M., Boller, Th., Krabbe, A., Blietz, M., Nakai, N., Wagner, S. J., & Stember, A. 1996, *ApJ*, 472, 588
- Elias, J. H., Frogel, J. A., Matthews, K., & Neugebauer, G. 1982, *AJ*, 87, 1029
- Engelbracht, C. W., Rieke, M. J., Rieke, G. H., & Latter, W. B. 1996, *ApJ*, 467, 227
- Engelbracht, C. W., Rieke, M. J., Rieke, G. H., Kelly, D. M., & Achtermann, J. M. 1998, *ApJ*, 505, 639
- Filippenko, A. V., & Sargent, W. L. 1985, *ApJS*, 57, 503
- Filippenko, A. V., & Sargent, W. L. 1988, *ApJ*, 324, 134
- Filippenko, A. V., & Terlevich, R. 1992, *ApJ*, 397, L79
- Forbes, D. A., Ward, M. J., DePoy, D. L., Boisson, C., & Smith, M. S. 1992, *MNRAS*, 254, 509
- García-Vargas, M. L., Bressan, A., & Díaz, A. I. 1995, *A&AS*, 112, 35
- Genzel, R., Weitzel, L., Tacconi-Garman, L. E., Blietz, M., Cameron, M., Krabbe, A., Lutz, D., & Sternberg, A. 1995, *ApJ*, 144, 129
- González-Delgado, M. R., & Pérez, E. 1996a, *MNRAS*, 281, 781
- González-Delgado, M. R., & Pérez, E. 1996b, *MNRAS*, 281, 1105
- Goodrich, R. W., Veilleux, S., & Hill, G. J. 1994, *ApJ*, 422, 521
- Heckman, T. M. 1980, *A&A*, 87, 152
- Heckman, T. M. 1986, in *IAU Sympos. 121, Observational Evidence of Activity in Galaxies*, ed. E. Ye. Khachikian, K. J. Fricke, & J. Melnick (Dordrecht: Kluwer), p.421
- Ho, L. C., Filippenko, A. V., & Sargent, W. L. 1993, *ApJ*, 417, 63
- Ho, L. C., Filippenko, A. V., & Sargent, W. L. 1995, *ApJS*, 98, 477
- Ho, L. C., Filippenko, A. V., & Sargent, W. L. 1996, *ApJ*, 462, 183
- Ho, L. C., Filippenko, A. V., & Sargent, W. L. 1997a, *ApJS*, 112, 315
- Ho, L. C., Filippenko, A. V., Sargent, W. L. & Peng, C. Y. 1997b, *ApJS*, 112, 391
- Ho, L. C., Filippenko, A. V., & Sargent, W. L. 1997c, *ApJ*, 487, 568
- Hummer, D. G., & Storey, P. J. 1987, *MNRAS*, 224, 801
- Jones, H. R. A., Longmore, A. J., Allard, F., & Hauschildt, P. A. 1996, *MNRAS*, 280, 777
- Jones, H. R. A., Longmore, A. J., Jameson, R. F., & Mountain, C. M. 1994, *MNRAS*, 267, 413
- Keel, W. C. 1983, *ApJ*, 269, 466
- Keel, W. C. 1996, *PASP*, 108, 917
- Keel, W. C., Kennicutt, R. C. Jr., Hummel, B., & van der Hulst, J. M. 1985, *AJ*, 90, 708
- Kirkpatrick, J. D., Kelly, D. M., Rieke, G. H., Liebert, J., Allard, F., & Wehrse, R. 1993, *ApJ*, 402, 643
- Koratkar, A., Deustua, S. E., Heckman, T., Filippenko, A. V., Ho, L. C., & Rao, M. 1995, *ApJ*, 440, 132
- Larkin, J. E., Armus, L., Knop, R. A., Soifer, B. T., & Matthews, K. 1998, *ApJ*, 493, 59
- Leitherer, C., & Heckman, T. M. 1995, *ApJS*, 96, 9
- Leitherer, C., Schaerer, D., Goldader, J. D., González-Delgado, R. M., Robert, C., Foo Kune, D., de Mello, D. F., Devost, D., & Heckman, T. M. 1999, *ApJS*, 123, 3
- Livingston, W., & Wallace L. 1991, in *Atlas of the Solar Spectrum in the Infrared from 1850 to 9000 cm⁻¹ (1.1 to 5.4 μm)*, N.S.O. Technical Report # 91-001
- Lumsden, S. L., & Puxley, P. J. 1995, *MNRAS*, 276, 723
- Maiolino, R., Rieke, G. H., & Rieke, M. J. 1996, *AJ*, 111, 537
- Maoz, D., Filippenko, A. V., Ho, L. C., Rix, H.-W., Bahcall, J. N., Schneider, D. P., & Macchetto, F. D. 1995, *ApJ*, 440, 91
- Maoz, D., Koratkar, A., Shields, J. C., Ho, L. C., Filippenko, A. V., & Sternberg, A. 1998, *AJ*, 116, 55
- McLeod, K. K., Rieke, G. H., Rieke, M. J., & Kelly, D. M. 1993, *ApJ*, 412, 111
- Mouri, H., Nishida, M., Taniguchi, Y., & Kawara, K. 1990, *ApJ*, 360, 55
- Nussbaumer, H., & Storey, P. J. 1988, *A&A*, 193, 327
- Oliva, E., & Origlia, L. 1992, *A&A*, 254, 466
- Rieke, G. H., Loken, L., Rieke, M. J., & Tamblyn, P. 1993, *ApJ*, 412, 99
- Rix, H.-W. R., Kennicutt, R. C. Jr., Braun, R., & Waltherbos, R. A. M. 1995, *ApJ*, 438, 155
- Shields, J. C., & Kennicutt, R. C. Jr. 1995, *ApJ*, 454, 808
- Shields, J. C. 1992, *ApJ*, 399, L27
- Simpson, C., Forbes, D. A., Baker, A. C., & Ward, M. J. 1996, *MNRAS*, 283, 777
- Smith, R.C., Kirshner, R. P., Blair, W. P., Long, K. S., & Winkler, P. F. 1993, *ApJ*, 407, 564
- Spinoglio, L., Malkan, M. A., Rush, B., Carrasco, L., & Recillas-Cruz, E. 1995, *ApJ*, 453, 616
- Stasińska, G., & Leitherer, C. 1996, *ApJS*, 107, 661
- Stauffer, J. R. 1982, *ApJ*, 262, 66
- Striganov, A. R., & Sventiskii, N. R. 1968, in *Tables of Spectral Lines of Neutral and Ionized Atoms*, IF/PLENUM, New York-Washington
- Tadhunter, C. N., Morganti, R., di Serego Alighieri, S., Fosbury, R. A. E., & Danziger, I. J. 1993, *MNRAS*, 259, 709
- Taniguchi, Y., Ohyama, Y., Yamada, T., Mouri, H., & Yoshida, M. 1996, *ApJ*, 467, 215
- Vacca, W. D., Garmany, C. D., & Shull, J. M. 1996, *ApJ*, 460, 914
- Vanzi, L., Rieke, G. H., Martin, C. L., & Shields, J. C. 1996, *ApJ*, 466, 150
- Vanzi, L., & Rieke, G. H. 1997, *ApJ*, 479, 694
- Vanzi, L., Alonso-Herrero, A., & Rieke, G. H. 1998, *ApJ*, 504, 94
- Veilleux, S., & Osterbrock, D. E. 1987, *ApJS*, 63, 295
- Veilleux, S., Kim, D. -C., Sanders, D. B., Mazzarella, J. M., & Soifer, B. T. 1995, *ApJS*, 98, 171
- Veilleux, S., Goodrich, R. W., & Hill, G. J. 1997, *ApJ*, 477, 631
- Véron-Cetty, M. -P., & Véron, P. 1986, *A&AS*, 66, 335
- Véron, P., Goncalves, A. C., & Véron-Cetty, M. -P. 1997, *A&A*, 319, 52
- Walker, C. E., Lebofsky, M. J., & Rieke, G. H. 1988, *ApJ*, 325, 687
- Williams, D. M., Thompson, C. L., Rieke, G. H., & Montgomery, E. F. 1993, *Proc. SPIE*, 1946, 482

In this appendix we discuss the properties of the sample of LINERs presented in this paper together with those additional LINERs for which there is significant evidence for the starburst activity to be related with the LINER activity.

INDIVIDUAL OBJECTS

NGC 253.— The properties of this galaxy are extensively discussed in Engelbracht et al. (1998). Its optical line ratios place it as a transition object between pure starburst and weak-[O I] LINERs. As shown in Engelbracht et al. (1998) and here, the optical line ratios of this galaxy are consistent with photoionization by stars with $T = 38,000$ K and some contribution from SNRs. Therefore the LINER characteristics of this galaxy are entirely explained by the presence of a starburst.

NGC 404.— The optical line ratios in this galaxy (Ho et al. 1993) meet Heckman (1980) definition for LINERs. No broad component of $H\alpha$ is detected (Ho et al. 1997b). The location in the optical ratio diagnostic diagrams places this galaxy in the transition object region. Evidence for star-formation in this galaxy comes from both the young underlying stellar population and the circumnuclear H II region-type emission in its optical spectrum (Ho et al. 1993, 1995). In addition the UV ionizing source in this galaxy is a star cluster slightly older than the one in NGC 4569 (Maoz et al. 1998), as also suggested by the higher SNR contribution than in NGC 4569 needed to reproduce the $[\text{Fe II}]1.257 \mu\text{m}/\text{Pa}\beta$ line ratio and optical line ratios (Table 7 and Figures 7 and 8). NGC 404 falls in the starburst-dominated LINER category.

NGC 1052.— This galaxy is the “prototypical” LINER. NGC 1052 is now known to show broad Balmer lines in polarized light (Barth et al. 1999), which makes it another AGN-dominated LINER. The properties of this LINER together with the infrared spectroscopy were discussed in detail in Alonso-Herrero et al. (1997).

NGC 2639.— The optical line ratios (Ho et al. 1993) of NGC 2639 are very close to Heckman’s definition of LINER. The presence of a broad $H\alpha$ component in this galaxy has long been known (Keel 1983; Huchra et al. 1982; Ho et al. 1997a). The $[\text{Fe II}]1.257 \mu\text{m}$ line emission is very strong with $\text{Pa}\beta$ being observed probably in absorption. It shows the highest $[\text{Fe II}]1.257 \mu\text{m}/\text{Pa}\beta$ line ratio in our sample, in good accordance with the high $[\text{O I}]\lambda 6300/H\alpha$ line ratio. This galaxy is a good example of AGN-dominated LINER. Note that this galaxy contradicts Larkin et al. (1998) claim that LINERs with high $[\text{Fe II}]1.257 \mu\text{m}/\text{Pa}\beta$ ratio are starburst-dominated LINERs.

NGC 3031 (M81).— The LINER M81 is one of the best candidates for low-luminosity AGN (i.e., AGN-dominated LINER in our classification). Its properties in the UV and optical have been recently studied in great detail by Ho et al. (1996). Our J -band spectrum shows $[\text{Fe II}]1.257 \mu\text{m}$ emission embedded in a very strong underlying stellar continuum. The $[\text{Fe II}]$ emission must be very localized at the center of the galaxy, since the off-nucleus spectrum (see Figure 2) shows no emission from this line. The $\text{Pa}\beta$ line is probably seen in absorption. Due to the radial velocity of this galaxy, a small error in the correction for the $\text{Pa}\beta$ emission introduced by the division by the standard star can affect the detection of a very faint $\text{Pa}\beta$ emission from M81.

NGC 3367.— NGC 3367 is of special interest because its optical line ratios do not correspond to those of an H II region photoionized by hot stars, or a Seyfert 2 or a LINER (Dekker et al. 1988). The presence of a broad component of $H\alpha$ is not clear, due to important asymmetries (Ho et al. 1997b). In the optical it shows evidence for the presence of Wolf-Rayet emission features (Ho et al. 1995). This galaxy shows one of the lowest $[\text{Fe II}]1.257 \mu\text{m}/\text{Pa}\beta$ line ratios in our sample, giving indication for youth of the star-formation process. The upper limit to the $\text{He I}/\text{Br}10$ line ratio sets an upper limit to the stellar temperature ($< 40,000$ K) which is in good agreement with the stellar temperature needed in the H II/SNR model to reproduce its optical line ratios. NGC 3367 is clearly a starburst-dominated transition object.

NGC 3504.— This galaxy has been classified as a weak-[O I] LINER (Ho et al. 1993) and as a H II region (Ho et al. 1997a). In Alonso-Herrero et al. (1997) we presented H and K -band spectroscopy of this galaxy and concluded that the LINER characteristics of NGC 3504 could be easily explained with the presence of a recent starburst. The age of the burst, based on the $[\text{Fe II}]1.257 \mu\text{m}/\text{Pa}\beta$ line ratio would be very similar to that of NGC 253. From Table 7 and Figure 8 it is clear that the optical line ratios of this galaxy are well reproduced with an H II region photoionized with stars with temperature $T = 38,000$ K without the presence of very hot stars.

NGC 3998.— The optical line ratios (Ho et al. 1993) of NGC 3998 meet the LINER definition. The detection of broad $H\alpha$ (see Ho et al. 1997b and references therein) makes NGC 3998 another candidate for AGN-dominated LINER. This galaxy is in common with Larkin et al. (1998) study of LINERs. Their measured $[\text{Fe II}]1.257 \mu\text{m}/\text{Pa}\beta$ line ratio is lower than ours. Comparing our spectrum with theirs, our detection of the $[\text{Fe II}]1.257 \mu\text{m}$ line has a higher signal to noise. Larkin et al. (1998) claimed that the $[\text{Fe II}]1.257 \mu\text{m}/\text{Pa}\beta$ ratio was significantly lower in comparison with the $[\text{O I}]\lambda 6300/H\alpha$ ratio. However with our $[\text{Fe II}]1.257 \mu\text{m}/\text{Pa}\beta$ line ratio measured from the stellar continuum subtracted spectrum, the galaxy fits perfectly in the *correlation* (see Figure 6). NGC 3998 is another example of AGN-dominated LINER.

NGC 4569 (M90).— The optical line ratios of this galaxy given in Stauffer (1982) comply with Heckman definition of LINERs, however, it is classified as a transition object in Ho et al. (1997a) based on both its location in the diagnostic diagrams and the non detection of a broad component of $H\alpha$ (Ho et al. 1997b). The HST/UV spectrum of this galaxy (as in NGC 404) shows absorption line signatures indicative of a continuum dominated by light from massive stars (Maoz et al. 1998), and the HST/UV imaging shows extended emission (Barth et al. 1998). Keel (1996) in a detailed study of the UV and optical properties reaches the conclusion that a population of young stars is responsible for the properties of NGC 4569, although an extra component associated with either an AGN or a population of older stars is still necessary. Our J and H -band spectra show that the emission is strongly dominated by the underlying stellar continuum. The $\text{Pa}\beta$ line is clearly detected in emission. All this evidence leads to a classification of starburst-dominated LINER.

NGC 4579.— The optical line ratios of this galaxy (González-Delgado & Pérez 1996b) satisfy only one of the criteria in Heckman’s definition ($[\text{O II}]\lambda 3727/[\text{O III}]\lambda 5007 = 1.53$). However the position of the line ratios in the diagnostic diagrams

is in the overlapping region of LINERs and Seyferts which lead Ho et al. (1997a) to classify this galaxy as a Seyfert 1.9 or LINER 1.9. The AGN-dominated nature of this LINER is confirmed by the detection of broad wings in the $H\alpha$ line (Filippenko & Sargent 1985; Ho et al. 1997b) along with broad lines in the UV (Maoz et al. 1998). NGC 4579 is the only galaxy in our sample with a FWHM of the $[\text{Fe II}]1.257\ \mu\text{m}$ line well above the instrument resolution. The J -band spectrum does not show $\text{Pa}\beta$ in emission.

NGC 4736 (M94).— This *true* LINER, according to Heckman (1980) definition, is an interesting example that suggests a combination of excitation mechanisms. The stellar continuum subtracted optical spectrum shows characteristics of a transition object (Ho et al. 1995), or type-2 LINER (Ho et al. 1997a), rather than a classical LINER. It does not show a broad component of $H\alpha$ (Ho et al. 1997b). This LINER has strong Balmer optical and infrared absorptions (e.g., Larkin et al. 1998) and other characteristics that make it the prototype of a late-phase starburst (e.g., Walker, Lebofsky, & Rieke 1988; Taniguchi et al. 1996), but also has a compact X-ray source possible indicative of a weak AGN (Cui, Feldkuhn, & Braun 1997). The high value of the $[\text{Fe II}]1.257\ \mu\text{m}/\text{Pa}\beta$ line ratio (Larkin et al. 1998) confirms the presence of an evolved starburst in which the SNRs have a dominant contribution.

NGC 4826 (M64).— This galaxy satisfies the LINER definition of Heckman (1980), however it is located in the region between transition objects and LINERs in Ho et al. (1997a) diagrams. No broad $H\alpha$ component is detected (Ho et al. 1997b). The range of optical line ratios measured by Keel (1983) and Ho et al. (1997a) are well reproduced with our model of H II region and SNRs. This fact seems to indicate that NGC 4826 is a starburst-dominated LINER. In addition, this galaxy shows a chain of H II regions near the center and evidence for shock-excited gas some 4 arcseconds off the nucleus (identified as a SNR by Rix et al. 1995).

NGC 5953.— This is an Sa pec galaxy interacting with the LINER/starburst galaxy NGC 5954. The determination of the activity class of the nucleus of this galaxy has been somehow problematic. It has been classified as a LINER by Veilleux et al. (1995), and as a Seyfert 2 by González-Delgado & Pérez (1996a). Note that some of optical line ratios reported for this galaxy in these two works differ by a factor of two. Using the reddening corrected optical line ratios given in Keel et al. (1985) and Veilleux et al. (1995), and the diagnostic diagrams, we find that NGC 5953 is located in the region occupied by both LINERs and transition objects. It shows strong circumnuclear star-formation activity as inferred from both 2D optical spectroscopic data (González-Delgado & Pérez 1996a; Véron, Gonçalves & Véron-Cetty 1997) and *HST*/UV images (Colina et al. 1997). Our J -band spectrum shows strong $[\text{Fe II}]$ and $\text{Pa}\beta$ emission lines. The ratio $[\text{Fe II}]1.2567\ \mu\text{m}/\text{Pa}\beta$ decreases for the large aperture (Table 5) which is an indication for an increased star-formation activity in the circumnuclear regions as seen in the optical. H and K -band spectroscopy of the companion NGC 5954 is presented in Vanzì, Alonso-Herrero, & Rieke (1998).

NGC 6764.— This SBb galaxy is classified as a classical LINER galaxy (i.e., satisfies Heckman’s definition). It shows Wolf-Rayet star features in its optical spectrum (Eckart et al 1996 and references therein), which makes this galaxy one of the most significant examples of starburst dominated classical LINER. The analysis of the starburst properties of this galaxy (Eckart et al. 1996) reveals that this galaxy is undergoing a burst of star-formation with a time scale of 10^7 yr consistent with the age derived from the $[\text{Fe II}]1.257\ \mu\text{m}/\text{Pa}\beta$ line ratio and EW of $\text{Br}\gamma$ (values taken from Calzetti 1997) in Figure 7.

NGC 7743.— The optical line ratio $[\text{O I}]\lambda 6300/H\alpha$ of NGC 7743 is typical of weak- $[\text{O I}]$ LINERs. However, when plotted in the diagnostic diagrams (Ho et al. 1994, 1997a), it lies close to the LINER/Seyfert 2 region. In the UV NGC 7743 is spatially extended (Barth et al. 1998). Its optical line ratios cannot be fitted with our H II-SNR model.